**NASA Technical Paper 2965**

1989

# Longitudinal Stability and Control Characteristics of the Quiet Short-Haul Research Aircraft (QSRA)

Jack D. Stephenson
and Gordon H. Hardy
*Ames Research Center*
*Moffett Field, California*

NASA
National Aeronautics and Space Administration
Office of Management
Scientific and Technical Information Division

# NOMENCLATURE

| | |
|---|---|
| $a_X$ | longitudinal acceleration, g |
| $a_Z$ | normal acceleration, g |
| $C_D$ | drag coefficient |
| $C_{D_R}$ | ram drag coefficient |
| $C_L$ | lift coefficient |
| $C_m$ | pitching-moment coefficient |
| $C_{m_q}e$ | effective pitch damping derivative, per rad |
| $C_T$ | thrust coefficient |
| $C_X$ | longitudinal force coefficient |
| $C_Z$ | normal force coefficient |
| $\overline{c}$ | mean aerodynamic chord, ft |
| $g$ | acceleration of gravity |
| $I_X, I_Y, I_Z$ | moment of inertia about the X- Y- and Z-axis, slug-ft squared |
| $I_{XZ}$ | product of inertia, slug-ft squared |
| $M$ | Mach number |
| $\dot{M}$ | engine air mass flow rate, slugs/sec |
| $m$ | mass, slugs |
| $N$ | engine fan rpm, percent |
| $P_s$ | atmospheric pressure, $lb/ft^2$ |
| $p, q, r$ | roll, pitch, and yaw rates, rad per sec |
| $\overline{q}$ | dynamic pressure, $lb/ft^2$ |
| $S$ | wing area, $ft^2$ |
| $V$ | airspeed, ft/sec or knots |
| $W$ | gross weight, lb |
| $X_e$ | longitudinal distance (averaged) from engine inlets to the c.g. |
| $Z_e$ | vertical distance (averaged) from engine inlets to the c.g. |
| $\alpha$ | angle of attack, deg or rad |
| $\delta_i$ | elevator, spoiler or thrust control variable |
| $\delta_u$ | USB flap deflection, deg |
| $\xi_i$ | state or measurement variable |

## Subscripts

| | |
|---|---|
| $e$ | elevator |
| $o$ | initial condition |
| $i$ | indicated value |
| $s$ | direct lift control spoilers |

## Abbreviations

| | |
|---|---|
| $a.c.$ | aerodynamic center |
| $DLC$ | direct lift control |
| $MAC$ | mean aerodynamic chord, ft |
| $USB$ | upper-surface blown (flaps) |

Column headings identifying the stability derivatives in Table 1 through Table 6 refer to the following definitions.

$$\text{CXA} = \frac{dC_X}{d\alpha} \qquad \text{CZA} = \frac{dC_Z}{d\alpha} \qquad \text{CMA} = \frac{dC_m}{d\alpha}$$

$$\text{CXA2} = \frac{dC_X}{d\alpha^2} \qquad \text{CZA2} = \frac{dC_Z}{d\alpha^2} \qquad \text{CMA2} = \frac{dC_m}{d\alpha^2}$$

$$\text{CXCT} = \frac{dC_X}{dC_T} \qquad \text{CZCT} = \frac{dC_Z}{dC_T} \qquad \text{CMCT} = \frac{dC_m}{dC_T}$$

$$\text{CXDE} = \frac{dC_X}{d\delta_e} \qquad \text{CZDE} = \frac{dC_Z}{d\delta_e} \qquad \text{CMDE} = \frac{dC_m}{d\delta_e}$$

$$\text{CXQ} = \frac{dC_X}{d(\frac{q\bar{c}}{2V})} \qquad \text{CZQ} = \frac{dC_Z}{d(\frac{q\bar{c}}{2V})} \qquad \text{CMQ} = \frac{dC_m}{d(\frac{q\bar{c}}{2V})}$$

$$\text{CXAD} = \frac{dC_X}{d(\frac{\dot{\alpha}\bar{c}}{2V})} \qquad \text{CZAD} = \frac{dC_Z}{d(\frac{\dot{\alpha}\bar{c}}{2V})} \qquad \text{CMAD} = \frac{dC_m}{d(\frac{\dot{\alpha}\bar{c}}{2V})}$$

$$\text{CXDS} = \frac{dC_X}{d\delta_s} \qquad \text{CZDS} = \frac{dC_Z}{d\delta_s} \qquad \text{CMDS} = \frac{dC_m}{d\delta_s}$$

$$\text{CLDS} = \frac{dC_L}{d\delta_s} \qquad \text{CDDS} = \frac{dC_D}{d\delta_s}$$

$$\text{CXDE2} = \frac{dC_X}{d\delta_e^2} \qquad \text{CZDE2} = \frac{dC_Z}{d\delta_e^2} \qquad \text{CMDE2} = \frac{dC_m}{d\delta_e^2}$$

$$\text{CXA3} = \frac{dC_X}{d\alpha^3} \qquad \text{CZA3} = \frac{dC_Z}{d\alpha^3} \qquad \text{CMA3} = \frac{dC_m}{d\alpha^3}$$

$$\text{CLDS} = \frac{dC_L}{d\delta_s} = -\frac{dC_Z}{d\delta_s}cos\alpha + \frac{dC_X}{d\delta_s}sin\alpha$$

$$\text{CDDS} = \frac{dC_D}{d\delta_s} = -\frac{dC_X}{d\delta_s}cos\alpha - \frac{dC_Z}{d\delta_s}sin\alpha$$

In these headings, XCG is the c.g. location in percent MAC, and VE is the initial equivalent airspeed, knots

An effective damping-in-pitch derivative is defined as follows:

$$C_{m_q}e = \frac{dC_m}{d(\frac{q\bar{c}}{2V})} + \frac{dC_m}{d(\frac{\dot{\alpha}\bar{c}}{2V})}$$

# SUMMARY

Flight experiments have been conducted to evaluate various aerodynamic characteristics of the Quiet Short-Haul Research Aircraft (QSRA), an experimental aircraft that makes use of the upper-surface blown (USB) powered-lift concept. Time-history records from maneuvers performed with the aircraft in landing-approach and take-off configurations (with its stability augmentation system disengaged) were analyzed to obtain longitudinal stability and control derivatives and performance characteristics. The experiments included measuring the aircraft responses to variations in the deflection of direct-lift-control spoilers and to thrust variations, as well as to elevator inputs. Most of the results are given for the aircraft in a landing configuration with the USB flaps at 50°. For this configuration, if the static longitudinal stability is defined as the variation of the pitching-moment coefficient with the lift coefficient at a constant thrust coefficient, this stability decreases significantly with increasing angle of attack above 9°. Also, for this configuration, at small and negative angles of attack and high levels of thrust, the elevators and the horizontal stabilizer lost effectiveness owing to incipient stalling, but this occurred only during unsteady maneuvers and for brief time intervals.

# INTRODUCTION

The Quiet Short-Haul Research Aircraft (QSRA) is an experimental transport aircraft designed to study various characteristics of a configuration that employs the upper surface blown (USB) flap technology to achieve short take-off and landing (STOL) capability. Flight investigations with the aircraft during the past several years have demonstrated that this configuration offers such a capability, and that its design goals, including high usable lift coefficients, reduced noise levels, and effective controllability throughout its operating envelope have been realized. However, this aircraft, in common with other high-wing-loading STOL transports that use powered- lift technology, when operating in a landing approach configuration at low speeds, displays poor longitudinal stability and experiences large trim changes with variations in flap deflection angles and thrust. Because of this, these types of aircraft generally require stability and control augmentation to achieve satisfactory handling characteristics. For the design of some proposed augmentation systems, such as the one described in reference 1, it is necessary to have an accurate model of the aerodynamics of the basic aircraft. This report describes a flight investigation which provides information that is applicable to choices of the longitudinal stability and control characteristics to be incorporated into such a model.

Aerodynamic data have been available from tests of a large-scale wind tunnel model designed to represent the major features of this research aircraft; i.e., its wing, nacelle, and flap configurations, as well as its engine-exhaust flow characteristics. These tests covered a large range of thrust coefficients and angles of attack (refs. 2 and 3). Lift and drag data from early flight tests of the QSRA generally agreed with the wind tunnel measurements, but some significant differences were evident, differences apparently associated with different patterns of flow separation on the wing and flaps. The effects are seen in the differences in the variations with angle of attack of lift-curve slopes and aerodynamic center locations (of the wing-body components). Because of such differences, which were observed in results from early tests covering a rather limited range of flight conditions, it was concluded that flight measurements were needed for a larger range of conditions.

Results from a flight program designed to measure some of the lift and drag characteristics of the QSRA in proposed landing-approach and take-off configurations have been reported in references 4, 5, 6, and 7. These results were obtained from quasi-steady flight maneuvers, a procedure in which, after the pilot sets the configuration, the thrust level and a selected high airspeed, the speed is gradually decreased in a series of steps until some minimum speed or maximum angle of attack is reached. The aerodynamic characteristics of an aircraft can also be determined from dynamic maneuvers (for an example, see Gerlach (ref. 8)). The longitudinal characteristics of the QSRA presented in this report were obtained from such maneuvers generated as the responses to the pilot's application of elevator, throttle, or DLC spoiler inputs. A single maneuver covers a range of angles of attack and thrust coefficients in a relatively short time, thus the time needed to acquire flight data on a variety of configurations can be significantly decreased by employing such maneuvers rather than the quasi-steady tests. In addition, because this type of maneuver generates pitching velocities, airspeed variations, and normal accelerations, it allows the determination not only of static aerodynamic coefficients, but also of control effectiveness and dynamic stability derivatives. The dynamic maneuvers providing the data presented in this report were performed with the aircraft in three configurations, two corresponding to those for landing approaches and one for take-off. For one landing approach configuration, the flight program included tests at several levels of engine thrust and with several initial airspeeds.

Various parameter-estimation computation procedures are available to use in extracting stability derivatives and other aerodynamic information from the time history records of such maneuvers. To obtain the results presented in this report, the records were analyzed with a linear regression estimation procedure described in reference 9. In the equations used to represent the dynamic behavior of the aircraft, it was assumed that the accelerations varied linearly with each variable except angle of attack and (in several solutions) the elevator angle. In most of the calculations, a second order variation with angle of attack was assumed, but for a few of the maneuvers, better results were obtained when a third order expression was assumed for the angle of attack variation.

# THE RESEARCH AIRCRAFT

The QSRA is a high wing transport designed and fabricated under contract to NASA by the Boeing Aircraft Company. It is a highly modified deHavilland C-8A Buffalo on which the original wing and engines were replaced with a new propulsive-lift wing and four nacelle-mounted Lycoming YF-102 turbofan engines. The mixed flow comprising the engine exhaust and fan efflux is directed over trailing- edge flaps behind the nacelles to increase the circulation lift and, when the flaps are deflected, to provide thrust vectoring. In addition to these USB flaps, the wing is fitted with conventional slotted flaps extending from 47 percent to 70 percent of the semispan. When the slotted flaps are deflected, the ailerons, which are provided with bleed-air boundary-layer control, are symmetrically drooped. Fixed leading-edge flaps extend from the outboard nacelles to the wing tips.

Spoilers located on the wing upper surface ahead of the slotted flaps provide two types of control functions. Besides augmenting the aileron lateral control, they can be symmetrically actuated to provide direct lift control. The spoilers consist of two surfaces on each wing, an inboard panel extending spanwise from 48 to 59 percent semispan and an outboard panel from 59 to 71 percent semispan. One of the maneuvers in the program described here was performed with only the outboard spoilers active, the inner panels being undeflected. The pilot's cockpit control allows the spoilers to be deflected at rates of up 50 degrees per second for direct lift control.

Figure 1 presents a sketch of the aircraft and various physical characteristics of its major components and control surfaces. Figure 2 is a photograph showing the aircraft in a landing approach configuration. Angle-of-attack and sideslip vanes are mounted on the nose boom, which also contains the apparatus for pitot-static measurements. Other measurements were taken from rate and attitude gyros, linear accelerometers, and transducers for measuring positions of all control surfaces, engine variables, and ambient air conditions. Data from these instruments were recorded at a rate of 100 Hz on board the aircraft and simultaneously at a ground station via telemetry. All of the measurements except those on which the thrust calculations were based were made with two independent sets of instrumentation. One set had been installed when the aircraft was delivered by the manufacturer (Boeing Co.) and is identified in this report as the analog set. The other, called the digital or Sperry set, was installed as part of a research program to investigate various control augmentation systems employing a flight-control digital computer. There were always some differences in the measurements between the two sets, usually caused by instrument biases. In a few cases there was major noise contamination of one or more of the analog variables, so that the availability of an alternate set allowed the data to be reduced and analyzed. The digital accelerometer records always had significantly less random noise, which may have been the result of a difference in the mountings of the instruments, i.e., better isolation of structural vibration with the digital instrument. The cycle time of the on-board computer required that the digital data be recorded at 20 Hz. Although processing of the analog data could take advantage of a higher frame rate, some early comparisons of the results of analysis using rates of 50 and 20 indicated that there was very little improvement from using the higher rates. For this reason, all of the analyses for both sets of data are based on the 20-Hz data rate.

Among the various flight maneuvers, the aircraft gross weight ranged from 43,000 to 58,000 lb, depending upon the amount of fuel on board at the time during a flight when the test was conducted. Figure 3 shows the c.g. location and the moment of inertia about the pitch axis as functions of weight.

AERODYNAMIC DATA

| | WING | HORIZ | VERT |
|---|---|---|---|
| AREA (TRAP), $ft^2$ | 600.0 | 233.0 | 152.0 |
| SPAN,ft | 73.5 | 32.0 | 14.0 |
| ASPECT RATIO | 9.0 | 4.4 | 1.22 |
| TAPER RATIO | 0.30 | 0.75 | 0.60 |
| SWEEP, C4, deg | 15.0 | 3.0 | 18.0 |
| MAC in. | 107.4 | 88.0 | 137.0 |
| CHORD ROOT, in. | 150.7 | 100.0 | 168.0 |
| CHORD TIP, in. | 45.2 | 75.0 | 100.0 |
| T/C BODY SIDE, % | 18.54 | 14 | 14 |
| T/C TIP, % | 15.12 | 12 | 14 |
| INCIDENCE, deg | 4.5 | – | – |
| DIHEDRAL, deg | 0.0 | – | – |
| TAIL ARM, in. | – | 525.0 in. | 488.0 in. |
| VOL COEFF V | – | 1.898 | 0.1402 |

CONTROL SURFACES

| $ft^2$* | | BLOWN |
|---|---|---|
| AILERON | 32.2 | BLC |
| FLAPS INBD | 105.0 | USB |
| FLAPS OUTBD | 40.2 | NONE |
| SPOILERS | 33.7 | NONE |
| L.E. FLAPS | 54.3 | NONE |
| ELEVATOR | 81.6 | NONE |
| RUDDER | 60.8 | NONE |

*THEORETICAL RETRACTED AREA

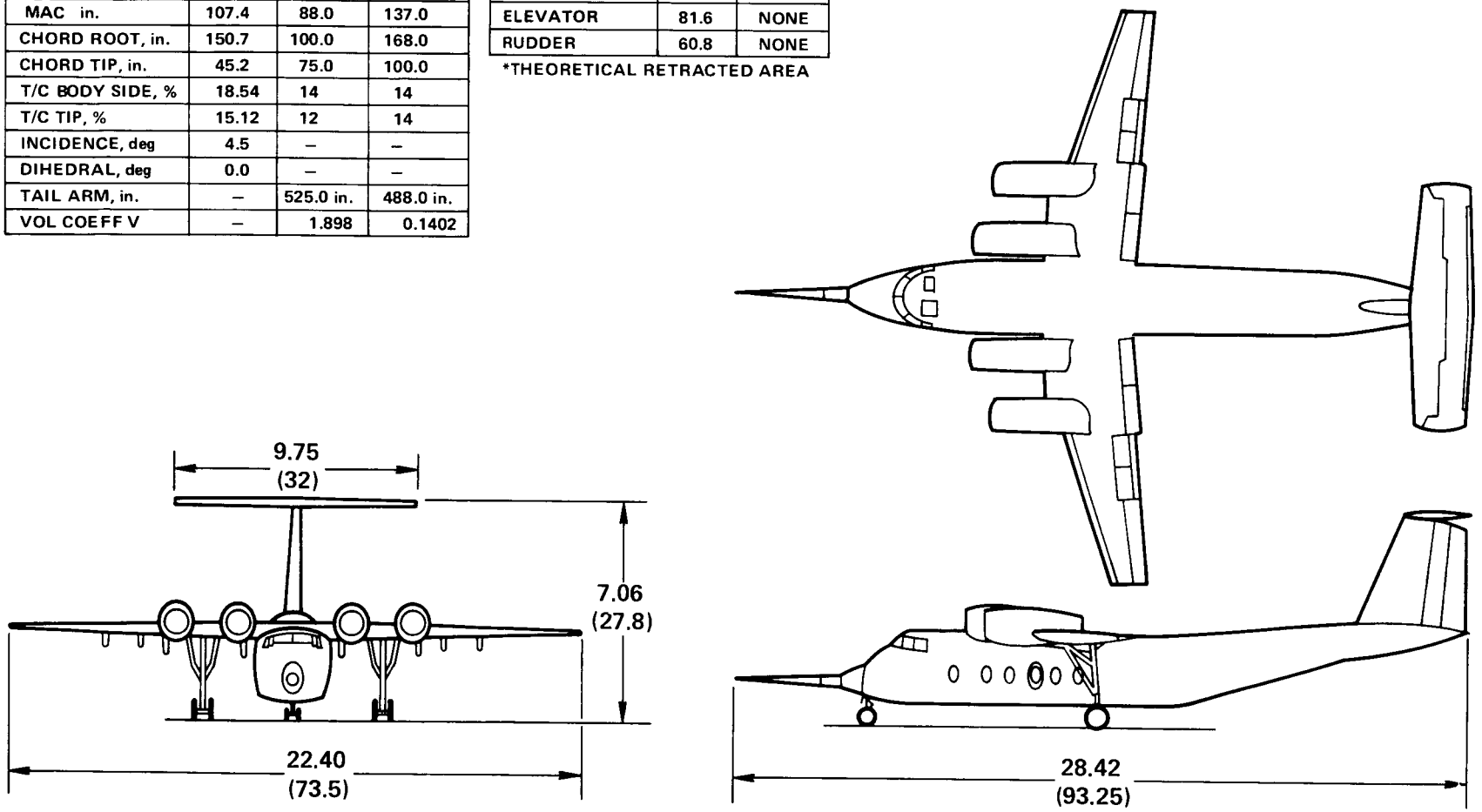


Figure 1. QSRA: general arrangement and dimensions.

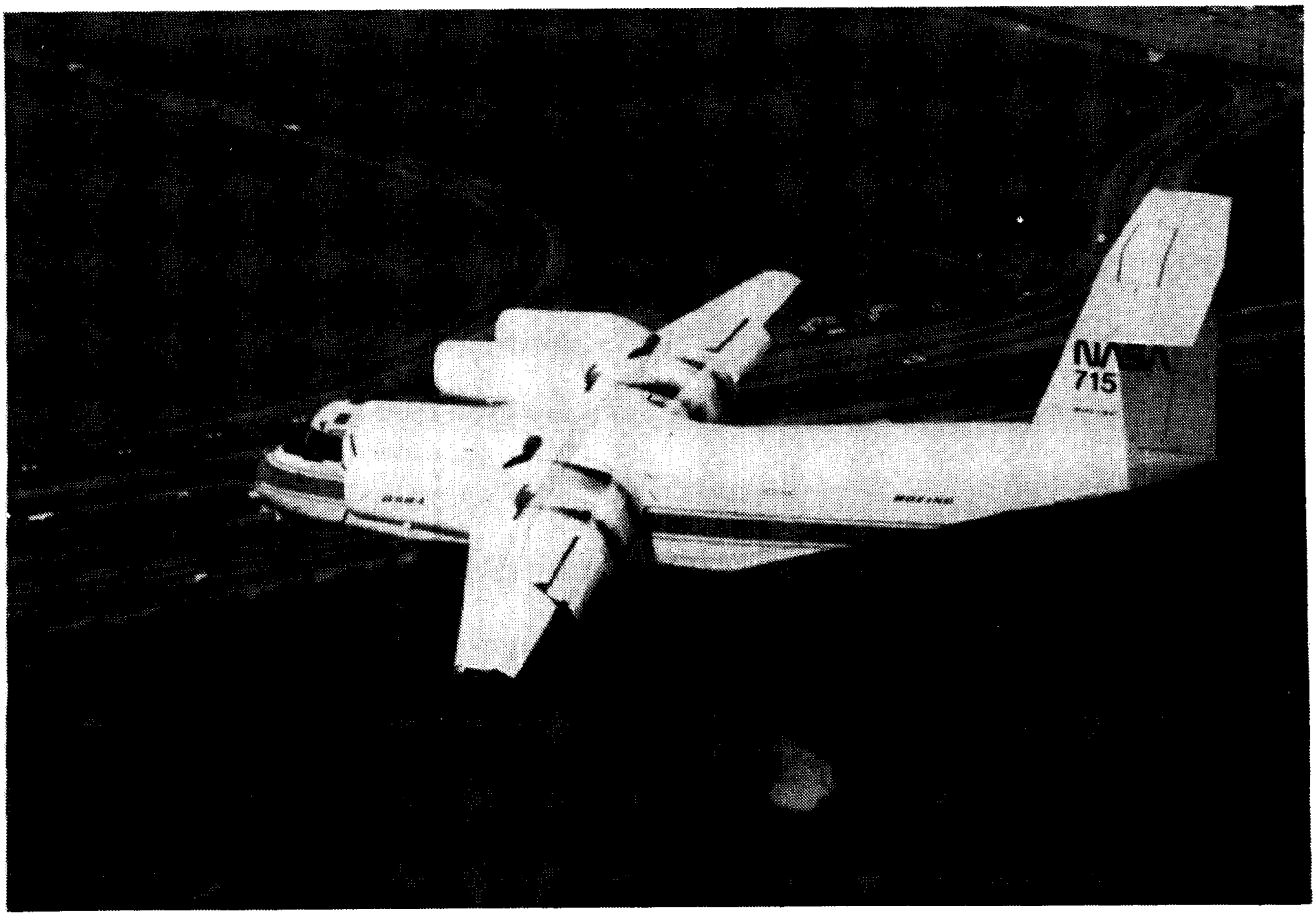


Figure 2. The QSRA aircraft in a landing approach configuration.

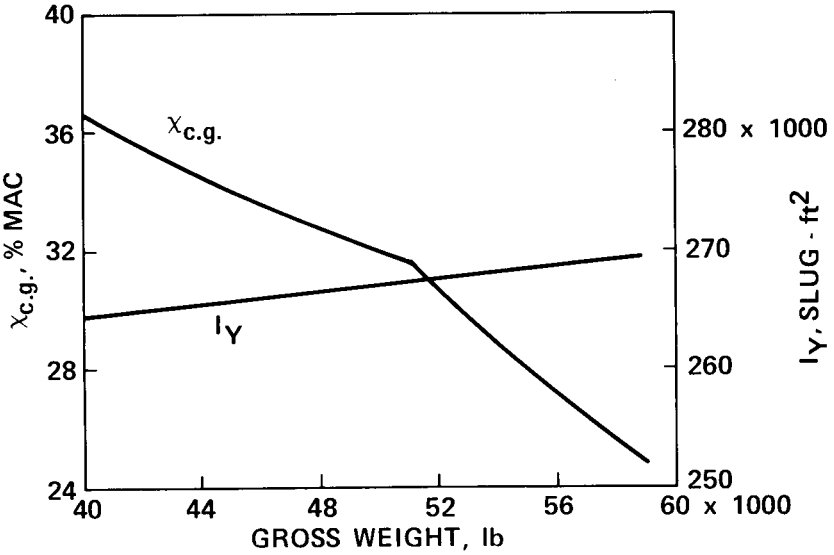


Figure 3. QSRA c.g. location and moment of inertia about the pitch axis vs. aircraft gross weight.

# FLIGHT EXPERIMENTS

Results presented in this report were obtained by analyzing time histories of variables recorded during longitudinal dynamic maneuvers produced by the various control inputs that the pilots applied: i.e., variation of the elevator angle, the direct lift control (DLC) spoiler angle, or the engine thrust. In a typical case the pilot was requested to first excite the motion with a throttle pulse and, after experiencing a response to this input, to excite a second response in the same maneuver with an elevator input. All of the tests were conducted with the slotted flaps set at (nominally) 59° and with the ailerons at 23° droop. For the majority of the tests, the DLC spoilers were not deflected and the USB flaps were set at 50°, an angle which in earlier tests was determined to be optimum for the QSRA during a landing approach. For a particular test maneuver, an initial airspeed or angle of attack was specified and the engine rpm was generally maintained at a constant specified fan speed, but as mentioned above, for some maneuvers the pilot briefly varied the engine speed as an input function. Figure 4 shows a typical set of time histories for one of these maneuvers. The flight program also included tests with another landing approach configuration (with the USB flaps at 66°) and with a configuration selected for good short take-off performance, for which the USB flaps were not deflected.

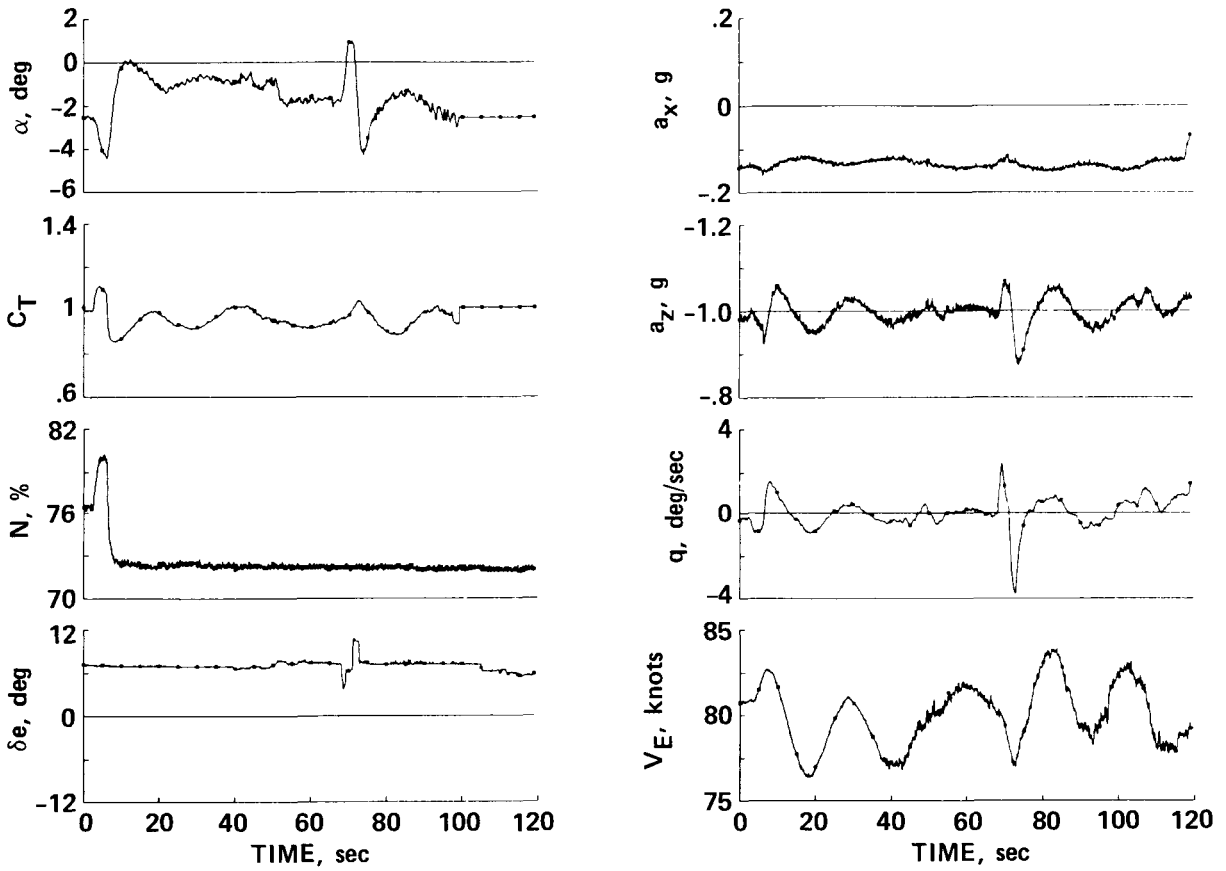


Figure 4. Typical time history record of a maneuver resulting from a thrust-change input followed by an elevator input. Maneuver B4.

Design studies of certain augmentation command and control systems for the QSRA and other powered-lift aircraft have included the assumption that the aircraft would have direct lift control capability. The QSRA design provides this capability by means of symmetrical actuation of its upper surface spoilers. In order for the spoilers to provide positive as well as negative changes in flightpath angle or airspeed, the spoilers must be set at reference angle of deflection. For the experiments described here, this angle was selected to be approximately 15° and the USB flaps were set at 50°. Data records from five maneuvers with the spoilers deployed have been analyzed. One maneuver was generated by two spoiler doublet inputs in sequence; two were the responses to a spoiler input followed by an elevator input; and three were produced by elevator inputs only.

In earlier studies (refs. 5 and 6), some aerodynamic characteristics of the QSRA were determined in flight with engine thrust levels corresponding to engine fan speeds ranging up to 89 percent. At the time the flights were conducted for the data in this report, however, the rpm of one engine was restricted to 85 percent. In order to represent the aircraft in a condition typical of its normal expected operation, that is, with all engines providing about the same thrust, this maximum rpm limitation was applied to all of the engines throughout this flight program.

# EQUATIONS OF MOTION

The following equations were used to represent the longitudinal motion of the aircraft, referred to body axes and assuming a rigid airframe. Linear accelerations are in gravitational units (g's) and are referred to the aircraft center of gravity (c.g.). Equations that transfer the measured accelerations to the c.g. are given in the appendix. Angular accelerations ($\dot{p}$, $\dot{q}$, and $\dot{r}$) in radians per second per second were calculated as the time derivatives of the roll, pitch, and yaw rates.

$$a_X \frac{mg}{\bar{q}S} = C_X - C_{D_R} \cos \alpha \tag{1}$$

$$a_Z \frac{mg}{\bar{q}S} = C_Z - C_{D_R} \sin \alpha \tag{2}$$

$$[I_y \dot{q} - (I_Z - I_X)pr - I_{XZ}(r^2 - p^2)] \frac{1}{\bar{q}\, S\, \bar{c}} = C_m + C_{D_R}\left(\frac{Z_e}{\bar{c}} \cos \alpha + \frac{X_e}{\bar{c}} \sin \alpha\right) \tag{3}$$

where $X_e$ and $Z_e$ are, respectively, the averages of the X- and Z-distances from the engine inlets to the c.g. The longitudinal and normal force coefficients are assumed to be given by the expressions

$$C_X = C_{X_o} + \sum_{i=1}^{5} \frac{dC_X}{d\xi_i} \xi_i + \sum_{j=1}^{6} \frac{dC_X}{d\delta_j} \delta_j \tag{4}$$

$$C_Z = C_{Z_o} + \sum_{i=1}^{5} \frac{dC_Z}{d\xi_i} \xi_i + \sum_{j=1}^{6} \frac{dC_Z}{d\delta_j} \delta_j \tag{5}$$

$$C_m = C_{m_o} + \sum_{i=1}^{5} \frac{dC_m}{d\xi_i} \xi_i + \sum_{j=1}^{6} \frac{dC_m}{d\delta_j} \delta_j \tag{6}$$

with the state and input variables defined as follows. The state variables are

$$\xi_1 = (\alpha - \alpha_o) \qquad \xi_2 = \frac{q\bar{c}}{2V}$$
$$\xi_3 = (\alpha - \alpha_o)^2 \qquad \xi_4 = \frac{\dot{\alpha}\bar{c}}{2V}$$
$$\xi_5 = (\alpha - \alpha_o)^3$$

and the input variables are

$$\delta_1 = (\delta_e - \delta_{e_o}) \qquad \delta_2 = (\delta_s - \delta_{s_o})$$
$$\delta_3 = (C_T - C_{T_o}) \qquad \delta_4 = \dot{C}_T$$
$$\delta_5 = \dot{\delta}_s \qquad \delta_6 = (\delta_e - \delta_{e_o})^2$$

# RESULTS

Table 1 through table 6 list the test conditions and aerodynamic stability derivatives obtained from the parameter estimation calculations. In table 1 the first three columns identify the flight maneuvers. The letter in the first column denotes a particular configuration. The letters A, B, and C denote, respectively, tests with USB flap deflection angles (column five) of 50°, 66°, and 0° with the DLC spoilers undeflected. Configurations D and E represent tests during which the spoilers were deflected and the USB flaps were at 49°. The tests designated as D1 through D5 differ from E1 in that the latter was done with only the two outboard spoiler panels deployed. The second and third columns in table 1 indicate the flight number and the order in which a particular maneuver was performed on that flight. The fourth column gives the code, either D or A, to indicate, respectively, whether the results were obtained by processing the set of data records from the Sperry digital or from the Boeing analog instrumentation. Also shown in table 1 for each maneuver are the following: the initial thrust coefficient and angle of attack; their ranges of variation during the maneuver; the aircraft c.g.; the initial normal-force, axial-force, and pitching-moment coefficents; and the initial equivalent airspeed. In computing the force and moment coefficients in this and the following tables, the contribution due to ram drag has been subtracted. Presentation of the coefficients without the ram drag contribution allows comparison of aerodynamic data obtained from maneuvers performed at different pressure altitudes and ambient temperaures.

Table 2 shows the following derivatives: normal and axial force coefficients and pitching-moment coefficients with respect to angle of attack, these same coefficients with respect to the $\alpha$ increment squared, and these coefficients with respect to the thrust coefficient, $C_T$. Table 3 shows the effectiveness of the DLC spoilers as calculated from the data representing the maneuvers mentioned earlier during which the spoilers, after having been set at an initial angle of approximately 15°, were actuated by the pilot so as to move to zero, then to about 28°, and back to 15°. In the table, the derivatives are given as force coefficients at constant angle of attack both in body axes and in lift and drag (stability) axes. The maneuver identified as E1 in the table was performed with the two inboard spoilers at zero deflection, so that only the two outboard spoilers were deflected and actuated during the test.

Table 4 presents the elevator effectiveness derivatives and derivatives with respect to pitch rate $q$ and angle-of-attack rate $\dot{\alpha}$. Where values are enclosed in parentheses, they were not obtained from the data analysis but instead were entered as fixed quantities. Earlier parameter estimation calculations performed to obtain the normal and axial forces due to elevator angle had indicated that in most cases the data records were not adequate to yield reliable values for these derivatives. In cases where the pitching-moment variation with elevator angle shown in the table was fixed, the maneuver was entirely the result of an engine thrust input by the pilot, so that there was no response to an elevator input. In the calculations to obtain the angle-of- attack rate and pitch rate derivatives, one or the other was fixed because of the well-known correlation of these variables. In the instances when both CZQ and CZAD are shown as fixed, there appeared to be insufficient excitation of the pitch rate to permit extraction of reliable values for these normal force derivatives.

Table 2 through table 4 show stability derivatives obtained when the data records were analyzed with the basic set of dynamic stability equations in which the forces and moments are assumed to vary linearly with elevator angle and as a second degree function of angle of attack. For several of the tests, it was found that improved agreement of the computed responses and the measurements could be obtained

Table 1. QSRA longitudinal dynamics tests. Initial conditions: $C_T$, $\alpha$, CZ, CX, CM, and VE; and minimum/maximum of $C_T$ and $\alpha$.

| RUN ID | FLT NO. AND RUN CODE | USB FLAP, DEG | THRUST COEF, $C_T$ | | | ALPHA, DEG | | | X CG %MAC | $CZ_0$ | $CX_0$ | $CM_0$ | VE, KT: INIT |
|---|---|---|---|---|---|---|---|---|---|---|---|---|---|
| | | | INIT | MIN | MAX | INIT | MIN | MAX | | | | | |
| A1 | 363 A D | 49.0 | 1.42 | 0.80 | 2.07 | -2.46 | -5.61 | 8.05 | 27.60 | -4.200 | 0.1540 | -0.0370 | 80.6 |
| A2 | 363 B D | 49.0 | 1.46 | 1.24 | 1.75 | -2.10 | -5.53 | 2.41 | 27.78 | -4.290 | 0.1770 | -0.0578 | 79.7 |
| A3 | 363 C D | 48.9 | 2.24 | 1.54 | 2.75 | 6.73 | -3.63 | 14.69 | 28.12 | -6.280 | 0.8310 | -0.1670 | 65.3 |
| A3 | 363 C A | 48.9 | 2.24 | 1.54 | 2.75 | 5.99 | -4.37 | 13.93 | 28.12 | -6.150 | 0.8420 | -0.1480 | " |
| A4 | 364 A D | 49.4 | 1.31 | 1.07 | 1.42 | -6.34 | -7.37 | -3.15 | 33.76 | -3.525 | 0.0501 | -0.0217 | 80.7 |
| A4 | 364 A A | 49.4 | 1.31 | 1.07 | 1.41 | -7.02 | -8.05 | -3.83 | 33.76 | -3.551 | 0.0357 | -0.0370 | " |
| A5 | 364 B D | 49.4 | 1.30 | 1.18 | 1.36 | -6.22 | -9.25 | -4.63 | 33.91 | -3.521 | 0.0447 | -0.0138 | 80.6 |
| A5 | 364 B A | 49.4 | 1.30 | 1.18 | 1.36 | -7.15 | -10.18 | -5.56 | 33.91 | -3.513 | 0.0247 | -0.0155 | " |
| A6 | 364 C D | 49.4 | 1.98 | 1.54 | 2.44 | 0.76 | -1.36 | 4.88 | 34.04 | -5.230 | 0.4620 | -0.1090 | 65.3 |
| A6 | 364 C A | 49.4 | 1.98 | 1.54 | 2.44 | 0.26 | -1.86 | 4.38 | 34.04 | -5.240 | 0.4710 | -0.1050 | " |
| A7 | 364 D D | 49.4 | 2.04 | 1.49 | 3.29 | 0.80 | -10.32 | 7.20 | 34.09 | -5.263 | 0.4880 | -0.1090 | 65.9 |
| A7 | 364 D A | 49.4 | 2.04 | 1.49 | 3.29 | 0.12 | -11.00 | 6.52 | 34.09 | -5.244 | 0.4860 | -0.0846 | " |
| A8 | 365 A D | 48.7 | 0.86 | 0.85 | 1.28 | 2.87 | 0.42 | 13.61 | 27.52 | -4.320 | 0.0497 | -0.0692 | 79.7 |
| A9 | 365 B D | 48.7 | 1.26 | 0.84 | 1.60 | 12.60 | 2.77 | 12.60 | 27.75 | -5.840 | 0.7250 | -0.1810 | 69.5 |
| A9 | 365 B A | 48.7 | 1.26 | 0.84 | 1.60 | 11.70 | 1.87 | 11.70 | 27.75 | -5.890 | 0.6820 | -0.1660 | " |
| A10 | 366 C D | 50.6 | 0.90 | 0.78 | 1.09 | 1.28 | -2.07 | 3.93 | 29.80 | -4.190 | -0.0253 | -0.0632 | 79.3 |
| A10 | 366 C A | 50.6 | 0.90 | 0.78 | 1.09 | 0.51 | -2.85 | 3.15 | 29.80 | -4.250 | -0.0647 | -0.0621 | " |
| A11 | 366 D D | 50.6 | 1.16 | 1.07 | 1.61 | 7.33 | 6.10 | 18.90 | 30.00 | -5.240 | 0.3300 | -0.1130 | 70.0 |
| A11 | 366 D A | 50.6 | 1.16 | 1.07 | 1.61 | 6.78 | 5.55 | 18.35 | 30.00 | -5.380 | 0.3100 | -0.1120 | " |
| B1 | 409 A D | 65.5 | 1.55 | 1.15 | 2.15 | 0.87 | -5.17 | 8.20 | 27.29 | -5.331 | -0.0445 | -0.0721 | 72.1 |
| B1 | 409 A A | 65.6 | 1.55 | 1.15 | 2.15 | 0.99 | -5.05 | 8.32 | 27.29 | -5.322 | -0.0938 | -0.0241 | " |
| B2 | 409 B D | 65.5 | 1.71 | 1.35 | 2.28 | 1.41 | -4.11 | 6.68 | 27.48 | -5.638 | 0.0008 | -0.1100 | 70.2 |
| B2 | 409 B A | 65.5 | 1.71 | 1.35 | 2.28 | 1.77 | -3.75 | 7.04 | 27.48 | -5.673 | -0.0405 | -0.1330 | " |
| B3 | 409 D D | 65.9 | 1.55 | 1.25 | 1.67 | 0.75 | -3.50 | 2.71 | 28.80 | -5.330 | -0.0476 | -0.1130 | 71.2 |
| B4 | 409 E D | 65.7 | 1.01 | 0.86 | 1.11 | -2.58 | -4.46 | 0.93 | 28.94 | -4.267 | -0.3326 | -0.0486 | 78.8 |
| B4 | 409 E A | 65.7 | 1.01 | 0.86 | 1.11 | -2.55 | -4.43 | 0.96 | 28.94 | -4.219 | -0.4078 | -0.0443 | " |
| C1 | 432 A D | -0.7 | 0.63 | 0.35 | 0.63 | 9.86 | 9.26 | 11.01 | 27.15 | -3.012 | 0.6882 | -0.1091 | 95.1 |
| C1 | 432 A A | -0.7 | 0.63 | 0.35 | 0.63 | 10.39 | 9.79 | 11.54 | 27.15 | -3.016 | 0.7032 | -0.1026 | " |
| C2 | 432 B D | -0.6 | 0.58 | 0.58 | 0.68 | 7.71 | 7.37 | 9.18 | 27.22 | -2.675 | 0.5612 | -0.0775 | 100.3 |
| C2 | 432 B A | -0.6 | 0.58 | 0.58 | 0.68 | 8.20 | 7.86 | 9.67 | 27.22 | -2.715 | 0.5607 | -0.0711 | " |

Table 1. Concluded.

| RUN ID | FLT NO. AND RUN CODE | USB FLAP, DEG | THRUST COEF, $C_T$ | | | ALPHA, DEG | | | X CG %MAC | $CZ_0$ | $CX_0$ | $CM_0$ | VE, KT: INIT |
|---|---|---|---|---|---|---|---|---|---|---|---|---|---|
| | | | INIT | MIN | MAX | INIT | MIN | MAX | | | | | |
| C3 | 432 C D | -0.6 | 0.65 | 0.63 | 0.77 | 9.86 | 9.37 | 13.55 | 27.29 | -2.983 | 0.7031 | -0.1190 | 95.5 |
| C3 | 432 C A | -0.6 | 0.65 | 0.63 | 0.77 | 10.15 | 9.66 | 13.84 | 27.29 | -3.002 | 0.7149 | -0.1209 | " |
| C4 | 488 A D | -0.4 | 1.07 | 0.96 | 1.15 | 10.29 | 7.43 | 12.50 | 28.88 | -3.116 | 1.1523 | -0.1010 | 86.8 |
| C4 | 488 A A | -0.4 | 1.07 | 0.96 | 1.15 | 10.70 | 7.84 | 12.91 | 28.88 | -3.370 | 1.2725 | -0.1153 | " |
| C5 | 488 B D | -0.6 | 1.17 | 1.08 | 1.39 | 12.21 | 7.24 | 13.72 | 29.02 | -3.571 | 1.2921 | -0.2004 | 84.6 |
| C5 | 488 B A | -0.6 | 1.17 | 1.08 | 1.39 | 12.60 | 7.63 | 14.11 | 29.02 | -3.627 | 1.4654 | -0.2071 | " |
| C6 | 488 C D | -0.6 | 1.20 | 0.55 | 1.33 | 10.86 | 6.66 | 12.17 | 29.27 | -3.366 | 1.1872 | -0.1780 | 86.4 |
| C6 | 488 C A | -0.6 | 1.20 | 0.55 | 1.33 | 11.14 | 6.94 | 12.45 | 29.27 | -3.406 | 1.2844 | -0.1683 | " |
| D1 | 432 D D | 48.5 | 0.88 | 0.86 | 1.05 | 9.44 | 6.64 | 11.40 | 27.56 | -4.782 | 0.3364 | -0.1124 | 75.4 |
| D1 | 432 D A | 48.5 | 0.88 | 0.86 | 1.05 | 10.17 | 7.37 | 12.13 | 27.56 | -4.849 | 0.3523 | -0.1395 | " |
| D2 | 432 E D | 48.8 | 1.06 | 0.97 | 1.22 | 8.03 | 6.52 | 11.49 | 28.04 | -4.882 | 0.3465 | -0.1249 | 74.2 |
| D2 | 432 E A | 48.8 | 1.06 | 0.97 | 1.22 | 8.16 | 6.65 | 11.62 | 28.04 | -4.890 | 0.3131 | -0.0890 | " |
| D3 | 432 F D | 48.8 | 0.97 | 0.94 | 1.09 | -3.23 | -6.46 | -0.28 | 28.34 | -3.153 | -0.0329 | -0.0503 | 93.0 |
| D3 | 432 F A | 48.8 | 0.97 | 0.94 | 1.09 | -3.38 | -6.61 | -0.43 | 28.34 | -3.158 | -0.0397 | -0.0380 | " |
| D4 | 488 D D | 48.4 | 1.53 | 1.30 | 1.79 | 3.10 | -0.48 | 3.97 | 29.65 | -4.637 | 0.4024 | -0.1165 | 75.0 |
| D4 | 488 D A | 48.4 | 1.53 | 1.30 | 1.79 | 3.45 | -0.13 | 4.32 | 29.65 | -4.697 | 0.4255 | -0.1251 | " |
| D5 | 488 E D | 48.4 | 1.55 | 1.50 | 1.75 | 3.01 | 0.44 | 4.72 | 29.77 | -4.648 | 0.4134 | -0.1069 | 74.7 |
| D5 | 488 E A | 48.4 | 1.55 | 1.50 | 1.75 | 2.92 | 0.35 | 4.63 | 29.77 | -4.619 | 0.4003 | -0.0677 | " |
| E1 | 402 A D | 48.7 | 1.45 | 1.20 | 1.71 | -2.30 | -5.50 | 0.95 | 33.66 | -4.293 | 0.0903 | -0.0610 | 73.3 |
| E1 | 402 A A | 48.7 | 1.45 | 1.20 | 1.71 | -2.56 | -5.76 | 0.69 | 33.66 | -4.304 | 0.1053 | -0.0748 | " |

Table 2. QSRA longitudinal dynamics. Normal force, axial force, and pitching moment derivatives with respect to $\alpha$, $\alpha^2$, and $C_T$.

| RUN ID | FLT NO. AND RUN CODE | INIT. $C_T$ | INIT. ALPHA | CZA | CXA | CMA | CZA2 | CXA2 | CMA2 | CZCT | CXCT | CMCT |
|---|---|---|---|---|---|---|---|---|---|---|---|---|
| A1 | 363 A D | 1.42 | -2.46 | -8.15 | 1.115 | -0.939 | 0.725 | 6.094 | 0.190 | -1.072 | 0.481 | -0.417 |
| A2 | 363 B D | 1.46 | -2.10 | -7.80 | 1.252 | -1.290 | 0.905 | 6.759 | -2.496 | -1.183 | 0.443 | -0.313 |
| A3 | 363 C D | 2.24 | 6.73 | -7.03 | 2.853 | -0.241 | 3.940 | 6.950 | 1.710 | -1.098 | 0.433 | -0.409 |
| A3 | 363 C A | 2.24 | 5.99 | -7.43 | 2.685 | -0.212 | 4.678 | 5.580 | 1.490 | -0.915 | 0.434 | -0.418 |
| A4 | 364 A D | 1.31 | -6.34 | -8.50 | -0.070 | -0.722 | -7.310 | 7.640 | -1.230 | -1.201 | 0.465 | -0.346 |
| A4 | 364 A A | 1.31 | -7.02 | -8.98 | 0.329 | -0.907 | -6.370 | 8.160 | 6.090 | -1.089 | 0.481 | -0.344 |
| A5 | 364 B D | 1.30 | -6.22 | -7.85 | 0.234 | -1.460 | 0.336 | 3.760 | 0.438 | -1.142 | 0.435 | -0.225 |
| A5 | 364 B A | 1.30 | -7.15 | -7.49 | 0.273 | -1.470 | 14.740 | 4.552 | -0.743 | -0.858 | 0.407 | -0.299 |
| A6 | 364 C D | 1.98 | 0.76 | -7.70 | 1.787 | -0.761 | -4.030 | 3.311 | 5.370 | -1.066 | 0.444 | -0.305 |
| A6 | 364 C A | 1.98 | 0.26 | -8.24 | 2.350 | -0.652 | -7.410 | 6.860 | 6.460 | -0.851 | 0.492 | -0.349 |
| A7 | 364 D D | 2.04 | 0.80 | -7.79 | 1.689 | -0.133 | -2.504 | 4.837 | -3.688 | -1.093 | 0.457 | -0.338 |
| A7 | 364 D A | 2.04 | 0.12 | -8.65 | 1.802 | 0.003 | -2.750 | 7.770 | -3.130 | -0.773 | 0.481 | -0.395 |
| A8 | 365 A D | 0.86 | 2.87 | -7.32 | 2.063 | -1.124 | 7.610 | 6.920 | 3.460 | -1.430 | 0.377 | -0.325 |
| A9 | 365 B D | 1.26 | 12.60 | -4.03 | 3.900 | 0.424 | 13.940 | 5.890 | 4.070 | -1.176 | 0.488 | -0.356 |
| A9 | 365 B A | 1.26 | 11.70 | -6.25 | 4.187 | 0.278 | 2.532 | 8.020 | 3.614 | -1.048 | 0.541 | -0.346 |
| A10 | 366 C D | 0.90 | 1.28 | -7.04 | 1.730 | -1.067 | -8.560 | 5.410 | 0.699 | -1.392 | 0.403 | -0.305 |
| A10 | 366 C A | 0.90 | 0.51 | -7.86 | 1.873 | -1.151 | 0.094 | 0.135 | -3.620 | -1.111 | 0.431 | -0.346 |
| A11 | 366 D D | 1.16 | 7.33 | -6.34 | 3.030 | -0.243 | 7.176 | 6.062 | 2.840 | -1.308 | 0.390 | -0.282 |
| A11 | 366 D A | 1.16 | 6.78 | -5.06 | 2.764 | -0.145 | -4.510 | 5.910 | 3.270 | -0.990 | 0.472 | -0.375 |
| B1 | 409 A D | 1.55 | 0.87 | -9.88 | 1.850 | -1.210 | -7.140 | 3.910 | 0.749 | -1.420 | 0.266 | -0.488 |
| B1 | 409 A A | 1.55 | 0.99 | -10.45 | 1.770 | -1.110 | 1.055 | 2.060 | 0.382 | -1.310 | 0.270 | -0.544 |
| B2 | 409 B D | 1.71 | 1.41 | -8.70 | 2.200 | -1.270 | -2.680 | 5.670 | -1.390 | -1.490 | 0.246 | -0.365 |
| B2 | 409 B A | 1.71 | 1.77 | -8.98 | 2.090 | -1.220 | 8.450 | 2.370 | -1.150 | -1.210 | 0.141 | -0.377 |
| B3 | 409 D D | 1.55 | 0.75 | -8.09 | 2.400 | -1.600 | 7.850 | 7.210 | -0.816 | -1.570 | 0.202 | -0.329 |
| B4 | 409 E D | 1.01 | -2.58 | -10.09 | 1.010 | -1.380 | 11.040 | 8.010 | -0.170 | -1.680 | 0.307 | -0.428 |
| B4 | 409 E A | 1.01 | -2.55 | -11.36 | 1.220 | -1.310 | 16.310 | 10.490 | -0.374 | -1.670 | 0.142 | -0.453 |
| C1 | 432 A D | 0.63 | 9.86 | -9.05 | 1.590 | -0.363 | (0.000) | 20.800 | -9.830 | -1.170 | 1.070 | -0.132 |
| C1 | 432 A A | 0.63 | 10.39 | -7.22 | 1.560 | -0.536 | -16.350 | 9.920 | -11.280 | -0.940 | 1.140 | -0.113 |
| C2 | 432 B D | 0.58 | 7.71 | -6.04 | 1.270 | -1.180 | (0.000) | 27.900 | -20.360 | -1.240 | 1.010 | -0.116 |
| C2 | 432 B A | 0.58 | 8.20 | -6.55 | 1.600 | -1.500 | (0.000) | 29.190 | -13.150 | -0.934 | 1.050 | -0.099 |

Table 2. Concluded.

| RUN ID | FLT NO. AND RUN CODE | INIT. $C_T$ | INIT. ALPHA | CZA | CXA | CMA | CZA2 | CXA2 | CMA2 | CZCT | CXCT | CMCT |
|---|---|---|---|---|---|---|---|---|---|---|---|---|
| C3 | 432 C D | 0.65 | 9.86 | -5.05 | 2.150 | -0.955 | -7.840 | 5.780 | -13.120 | -1.440 | 0.956 | -0.087 |
| C3 | 432 C A | 0.65 | 10.15 | -5.89 | 1.980 | -1.150 | -11.150 | 14.040 | - 7.920 | -1.050 | 1.070 | -0.139 |
| C4 | 488 A D | 1.07 | 10.29 | -5.92 | 2.549 | -1.600 | -18.550 | 15.59 | - 3.045 | -1.002 | 0.870 | -0.061 |
| C4 | 488 A A | 1.07 | 10.70 | -6.27 | 4.663 | -1.531 | -2.670 | (20.00) | 2.759 | -0.780 | 0.782 | -0.093 |
| C5 | 488 B D | 1.17 | 12.21 | -4.89 | 2.325 | -1.474 | 13.980 | 1.427 | 1.708 | -1.010 | 0.911 | -0.102 |
| C5 | 488 B A | 1.17 | 12.60 | -5.46 | 3.808 | -1.413 | 15.880 | 6.757 | 3.490 | -0.672 | 1.288 | -0.105 |
| C6 | 488 C D | 1.20 | 10.86 | -5.03 | 1.563 | -1.251 | 8.398 | -7.486 | 6.585 | -0.828 | 0.964 | -0.147 |
| C6 | 488 C A | 1.20 | 11.14 | -5.94 | 4.751 | -1.727 | 4.356 | 33.560 | - 3.020 | -0.734 | 1.058 | -0.112 |
| D1 | 432 D D | 0.88 | 9.44 | -5.01 | 3.154 | -0.292 | (0.000) | -5.647 | 10.560 | -1.972 | 0.409 | -0.159 |
| D1 | 432 D A | 0.88 | 10.17 | -4.90 | 2.860 | -0.338 | (0.000) | -5.190 | 12.360 | -1.794 | 0.515 | -0.177 |
| D2 | 432 E D | 1.06 | 8.03 | -6.95 | 3.030 | -0.701 | 5.610 | 10.420 | 2.980 | -1.720 | 0.450 | -0.215 |
| D2 | 432 E A | 1.06 | 8.16 | -7.99 | 2.690 | -0.590 | 18.230 | 6.570 | 2.630 | -1.180 | 0.453 | -0.305 |
| D3 | 432 F D | 0.97 | -3.23 | -5.60 | 1.160 | -1.170 | (0.000) | -6.470 | -9.810 | -1.600 | 0.363 | -0.203 |
| D3 | 432 F A | 0.97 | -3.38 | -4.26 | 1.000 | -1.210 | (0.000) | -13.570 | -7.110 | -1.430 | 0.538 | -0.175 |
| D4 | 488 D D | 1.53 | 3.10 | -8.48 | 2.180 | -1.069 | -23.940 | 5.849 | 12.510 | -1.392 | 0.454 | -0.207 |
| D4 | 488 D A | 1.53 | 3.45 | -7.59 | 1.593 | -0.985 | (0.000) | 13.590 | 11.76 | -1.334 | 0.691 | -0.253 |
| D5 | 488 E D | 1.55 | 3.01 | -7.70 | 2.118 | -1.295 | -1.638 | -3.042 | 8.024 | -1.406 | 0.432 | -0.215 |
| D5 | 488 E A | 1.55 | 2.92 | -8.32 | 2.203 | -1.605 | -3.013 | 5.977 | 3.287 | -0.834 | 0.435 | -0.295 |
| E1 | 402 A D | 1.45 | -2.30 | -8.34 | 1.050 | -1.060 | -5.450 | 8.070 | -13.080 | -1.370 | 0.396 | -0.184 |
| E1 | 402 A A | 1.45 | -2.56 | -9.18 | 1.040 | -1.020 | 2.240 | 6.340 | -6.410 | -1.140 | 0.451 | -0.255 |

Table 3. DLC spoiler effectiveness. USB flaps, 50°.

| RUN ID | FLT NO. AND RUN CODE | INIT. $C_T$ | INIT. ALPHA DEG | CZDS PER RAD | CXDS PER RAD | CMDS PER RAD | CLDS PER RAD | CDDS PER RAD |
|---|---|---|---|---|---|---|---|---|
| D1 | 432 D D | .88 | 9.44 | 2.04 | -.056 | .025 | -2.03 | -.300 |
| D1 | 432 D A | .88 | 10.17 | 2.32 | .025 | .005 | -2.28 | -.433 |
| D3 | 432 F D | .97 | - 3.23 | 1.42 | -.005 | .007 | -1.42 | .085 |
| D3 | 432 F A | .97 | - 3.38 | 1.24 | -.005 | -.021 | -1.24 | .075 |
| E1[a] | 402 A D | 1.45 | - 2.30 | .90 | -.046 | .031 | - .90 | .082 |
| E1[a] | 402 A A | 1.45 | - 2.65 | 1.17 | .018 | .025 | -1.16 | .034 |

[a]Only the two outboard spoilers were deployed during maneuver E1.

if one or both of two other terms were added to these equations. These terms make the accelerations functions of the elevator angle squared, and the third power of angle of attack. Table 5 presents the elevator pitching-moment effectiveness derivatives obtained when the second order elevator term was included in calculations for four of the maneuvers. There was no significant benefit in adding the terms to the normal or the axial force equations. Table 6 presents the force and pitching moment derivatives that resulted from using the third order angle-of-attack terms as well as the second order elevator-effectiveness term.

An important part of the determination of stability derivatives obtained by use of a parameter estimation procedure is the evaluation of levels of confidence in the accuracy of the estimates. In the flight program carried out to acquire data for this report, it was possible in some cases to improve the confidence levels by performing more than one maneuver at the same test conditions and obtaining similar results. Because the airplane had been furnished with two independent systems of flight data instrumentation, there was also a basis for an improved level of confidence when the estimates derived from both sources were in agreement. Some sources of errors were recognized as the commonly observed effects of the correlation of variables. These effects are discussed in the section on aerodynamic damping and elevator effectiveness. The time histories of the lift, drag and moment coefficients computed with the estimated parameter values were compared graphically with plots of these coefficients determined from the data measurements for all test maneuvers. In the case of one maneuver, the test identified as C1, a satisfactory match was not achieved. For the other solutions, the comparisons indicated that the computed variations agreed well with the measurements; an example is shown in figure 5.

Table 4. QSRA longitudinal dynamics. Normal force, axial force, and pitching moment derivatives with respect to elevator angle, pitch rate, and angle of attack rate.

| RUN ID | FLT NO. AND RUN CODE | INIT. $C_T$ | INIT. ALPHA DEG | CZDE PER RAD | CXDE PER RAD | CMDE PER RAD | CZQ PER RAD | CZAD PER RAD | CXQ PER RAD | CXAD PER RAD | CMQ PER RAD | CMAD PER RAD |
|---|---|---|---|---|---|---|---|---|---|---|---|---|
| A1 | 363 A D | 1.42 | -2.46 | (-0.70) | (0.10) | -2.69 | (-10.00) | -20.53 | - 3.83 | (0.00) | -38.94 | (-20.00) |
| A2 | 363 B D | 1.46 | -2.10 | (-0.70) | 0.28 | -3.33 | -8.78 | -2.00 | 2.29 | 2.00 | -41.20 | (-20.00) |
| A3 | 363 C D | 2.24 | 6.73 | (-0.66) | (0.10) | -3.23 | -22.91 | (-10.00) | -4.61 | (0.00) | -44.73 | (-20.00) |
| A3 | 363 C A | 2.24 | 5.99 | (-0.66) | (0.10) | -3.22 | -28.07 | (-10.00) | -5.88 | (0.00) | -51.30 | (-20.00) |
| A4 | 364 A D | 1.31 | -6.34 | (-0.70) | (0.10) | -3.31 | (-10.00) | -7.52 | 14.77 | (5.00) | -52.92 | (-20.00) |
| A4 | 364 A A | 1.31 | -7.02 | (-0.70) | (0.10) | -3.34 | (0.00) | -0.31 | 10.33 | (5.00) | -46.38 | (-20.00) |
| A5 | 364 B D | 1.30 | -6.22 | -0.80 | (0.10) | -3.15 | -3.26 | (0.00) | 6.18 | (3.00) | -32.09 | (-20.00) |
| A5 | 364 B A | 1.30 | -7.15 | -0.58 | 0.17 | -3.08 | (0.00) | 13.40 | (-5.00) | 22.06 | -41.07 | (-20.00) |
| A6 | 364 C D | 1.98 | 0.76 | (-0.70) | (0.10) | -3.16 | (-10.00) | -4.03 | (0.00) | 2.03 | -36.05 | (-20.00) |
| A6 | 364 C A | 1.98 | 0.26 | (-0.70) | (0.10) | -3.17 | (-5.00) | -0.58 | (0.00) | 3.20 | -43.73 | (-20.00) |
| A7 | 364 D D | 2.04 | 0.80 | (-0.70) | (0.10) | -2.95 | -19.13 | (-5.00) | 3.71 | (-5.00) | -44.22 | (-20.00) |
| A7 | 364 D A | 2.04 | 0.12 | (-0.70) | (0.10) | -2.99 | (-5.00) | (-5.00) | 1.05 | (5.00) | -56.25 | (-20.00) |
| A8 | 365 A D | 0.86 | 2.87 | (-0.70) | (0.10) | -3.50 | (-10.00) | -16.77 | (0.00) | -4.21 | -44.67 | (-20.00) |
| A9 | 365 B D | 1.26 | 12.60 | (-0.70) | (0.10) | -3.44 | -25.04 | (-5.00) | 5.16 | (0.00) | -41.84 | (-20.00) |
| A9 | 365 B A | 1.26 | 11.70 | (-0.70) | (0.10) | -3.56 | (-5.00) | 15.94 | 5.86 | (0.00) | 36.67 | (-20.00) |
| A10 | 366 C D | 0.90 | 1.28 | -0.53 | 0.14 | -3.44 | -13.92 | (-5.00) | 2.79 | (0.00) | -42.36 | (-20.00) |
| A10 | 366 C A | 0.90 | 0.51 | -0.74 | (0.10) | -3.29 | -6.39 | (0.00) | -1.76 | (0.00) | -45.36 | (-20.00) |
| A11 | 366 D D | 1.16 | 7.33 | -0.46 | 0.07 | -3.35 | (-10.00) | -29.94 | (0.00) | -2.90 | (-40.00) | -15.79 |
| A11 | 366 D A | 1.16 | 6.78 | -0.64 | 0.17 | -3.38 | (-10.00) | -16.46 | 2.71 | (0.00) | -49.31 | (-20.00) |
| B1 | 409 A D | 1.55 | 0.87 | (-0.70) | (0.10) | (-3.20) | (-10.00) | -8.64 | (0.00) | -0.43 | -55.12 | (-20.00) |
| B1 | 409 A A | 1.55 | 0.99 | (-0.70) | (0.10) | (-3.20) | -22.17 | (-10.00) | (0.00) | -12.71 | -65.04 | (-20.00) |
| B2 | 409 B D | 1.71 | 1.41 | (-0.70) | (0.10) | -2.49 | -3.14 | (-5.00) | 4.01 | (0.00) | -43.08 | (-10.00) |
| B2 | 409 B A | 1.71 | 1.77 | (-0.70) | (0.10) | -2.23 | (-10.00) | 15.21 | -11.24 | (0.00) | -43.89 | (-10.00) |
| B3 | 409 D D | 1.55 | 0.75 | (-0.70) | (0.10) | -3.29 | -6.67 | (0.00) | -4.70 | (-1.00) | -34.58 | (-20.00) |
| B4 | 409 E D | 1.01 | -2.58 | (-0.70) | (0.10) | -3.68 | ( -5.00) | 8.91 | 13.73 | (0.00) | -49.09 | (-20.00) |
| B4 | 409 E A | 1.01 | -2.55 | (-0.70) | (0.10) | -2.90 | (-10.00) | (0.00) | -17.23 | (0.00) | -45.64 | (-20.00) |
| C1 | 432 A D | 0.63 | 9.86 | (-0.70) | (0.10) | (-3.20) | ( -5.00) | 13.62 | (0.00) | -2.78 | (-10.00) | -0.30 |
| C1 | 432 A A | 0.63 | 10.39 | (-0.70) | (0.10) | (-3.20) | ( 0.00) | 12.10 | (0.00) | -9.21 | (-10.00) | 14.06 |
| C2 | 432 B D | 0.58 | 7.71 | (-0.70) | (0.10) | -2.65 | (-10.00) | (-5.00) | (5.00) | -6.35 | -30.73 | (-20.00) |
| C2 | 432 B A | 0.58 | 8.20 | (-0.70) | (0.10) | -2.83 | (-10.00) | (-5.00) | (5.00) | 11.24 | -24.53 | (-20.00) |

Table 4. Concluded.

| RUN ID | FLT NO. AND RUN CODE | INIT. $C_T$ | INIT. ALPHA DEG | CZDE PER RAD | CXDE PER RAD | CMDE PER RAD | CZQ PER RAD | CZAD PER RAD | CXQ PER RAD | CXAD PER RAD | CMQ PER RAD | CMAD PER RAD |
|---|---|---|---|---|---|---|---|---|---|---|---|---|
| C3 | 432 C D | 0.65 | 9.86 | (-0.70) | (0.10) | -3.42 | -26.23 | (-10.00) | -0.64 | (0.00) | -37.03 | (-20.00) |
| C3 | 432 C A | 0.65 | 10.15 | (-0.70) | (0.10) | -3.53 | (-10.00) | (-5.00) | -4.84 | (0.00) | -40.46 | (-20.00) |
| C4 | 488 A D | 1.07 | 10.29 | (-0.70) | (0.10) | -3.28 | (-10.00) | -7.08 | (-5.00) | -2.31 | (-40.00) | -10.98 |
| C4 | 488 A A | 1.07 | 10.70 | (-0.70) | (0.10) | -3.54 | (-10.00) | -4.75 | (-5.00) | 21.59 | (-40.00) | -11.67 |
| C5 | 488 B D | 1.17 | 12.21 | (-0.70) | (0.10) | -3.49 | (-10.00) | -22.83 | (0.00) | 0.27 | (-40.00) | -20.00 |
| C5 | 488 B A | 1.17 | 12.60 | (-0.70) | (0.10) | -3.32 | (-10.00) | -12.15 | (0.00) | -10.41 | (-40.00) | -10.89 |
| C6 | 488 C D | 1.20 | 10.86 | (-0.70) | (0.10) | -3.65 | -4.89 | (-5.00) | 16.60 | (0.00) | -48.10 | (-20.00) |
| C6 | 488 C A | 1.20 | 11.14 | (-0.70) | (0.10) | -3.37 | -21.58 | (-5.00) | -2.46 | (0.00) | -41.41 | (-20.00) |
| D1 | 432 D D | 0.88 | 9.44 | (-0.70) | (0.10) | (-3.20) | 0.34 | (0.00) | 1.03 | (0.00) | -32.29 | (-10.00) |
| D1 | 432 D A | 0.88 | 10.17 | (-0.70) | (0.10) | (-3.20) | (0.00) | (-10.00) | 8.93 | (0.00) | -17.54 | (-10.00) |
| D2 | 432 E D | 1.06 | 8.03 | (-0.70) | (0.10) | -3.78 | (-5.00) | 2.04 | 3.03 | (0.00) | -48.92 | (-20.00) |
| D2 | 432 E A | 1.06 | 8.16 | (-0.70) | (0.10) | -3.92 | 1.16 | (-10.00) | (5.00) | -6.00 | -55.98 | (-20.00) |
| D3 | 432 F D | 0.97 | -3.23 | (-0.70) | (0.10) | -3.43 | (-5.00) | 2.83 | (0.00) | -0.88 | -41.25 | (-10.00) |
| D3 | 432 F A | 0.97 | -3.38 | (-0.70) | (0.10) | -2.67 | (-10.00) | (-5.00) | 0.71 | (0.00) | (-30.00) | 4.51 |
| D4 | 488 D D | 1.53 | 3.10 | (-0.70) | (0.10) | -3.49 | (-10.00) | 0.39 | (0.00) | -2.33 | (-30.00) | -11.72 |
| D4 | 488 D A | 1.53 | 3.45 | (-0.70) | (0.10) | -3.60 | -33.52 | (-5.00) | 28.53 | (0.00) | -35.22 | (-20.00) |
| D5 | 488 E D | 1.55 | 3.01 | (-0.70) | (0.10) | -3.43 | (-10.00) | -0.35 | (0.00) | -2.96 | (-40.00) | -5.11 |
| D5 | 488 E A | 1.55 | 2.92 | (-0.70) | (0.10) | -3.56 | (-5.00) | -18.59 | (0.00) | 2.85 | (-40.00) | -9.81 |
| E1 | 402 A D | 1.45 | -2.30 | (-0.70) | (0.10) | -3.62 | -8.15 | (0.00) | 3.93 | (0.00) | -32.22 | (-20.00) |
| E1 | 402 A A | 1.45 | -2.56 | (-0.70) | (0.10) | -3.10 | (-5.00) | -4.75 | 5.61 | (0.00) | -43.91 | (-20.00) |

Table 5. QSRA longitudinal dynamics tests. Nonlinear elevator effectiveness $\frac{dC_m}{d\delta_e^2}$.

| RUN ID | FLT NO. AND RUN CODE | INIT. $C_T$ | INIT. ALPHA DEG | USB FLAP DEG | CMDE | CMDE2 |
|---|---|---|---|---|---|---|
| A1 | 363 A D | 1.42 | -2.46 | 49.0 | -2.78 | -4.09 |
| A3 | 363 C D | 2.24 | 6.73 | 48.9 | -2.89 | -3.09 |
| A3 | 363 C A | 2.24 | 5.99 | 48.9 | -3.05 | -1.59 |
| A7 | 364 D D | 2.04 | 0.80 | 49.4 | -2.72 | -3.51 |
| A7 | 364 D A | 2.04 | 0.12 | 49.4 | -2.74 | -2.72 |
| B2 | 409 B D | 1.71 | 1.41 | 65.5 | -2.44 | -2.74 |
| B2 | 409 B A | 1.71 | 1.77 | 65.5 | -2.28 | -1.68 |

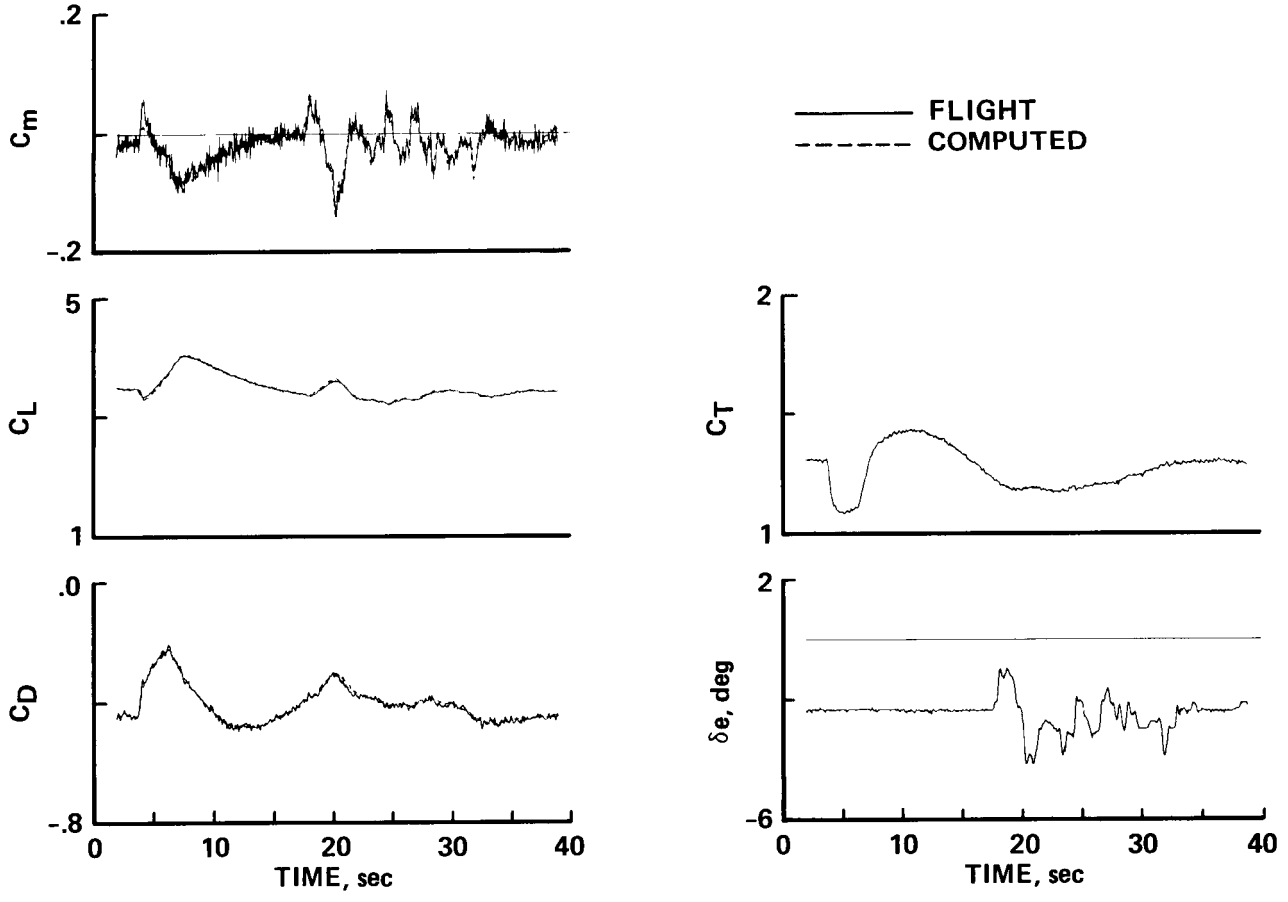


Figure 5. Comparison of computed and measured $C_D$, $C_L$, and $C_m$ time histories together with the corresponding $C_T$ and $\delta_e$ time histories.

Table 6. QSRA longitudinal dynamics tests. Normal force, axial force, and pitching moment derivatives with respect to $\alpha$, $\alpha^2$, and $\alpha^3$. USB flaps, 50°.

| RUN ID | FLT NO. AND RUN CODE | INIT. $C_T$ | INIT. ALPHA DEG | CZA | CXA | CMA | CZA2 | CXA2 | CMA2 | CZA3 | CXA3 | CMA3 |
|---|---|---|---|---|---|---|---|---|---|---|---|---|
| A1 | 363 A D | 1.42 | -2.46 | -8.130 | 1.12 | -1.04 | -0.47 | 6.56 | -2.75 | 6.48 | -2.80 | 20.50 |
| A3 | 363 C D | 2.24 | 6.73 | -7.112 | 2.65 | -0.26 | 3.77 | 8.83 | 2.95 | 1.83 | 27.63 | 3.73 |
| A3 | 363 C A | 2.24 | 5.99 | -7.277 | 2.35 | -0.21 | 3.75 | 7.56 | 1.92 | -17.00 | 36.50 | -0.68 |
| A6 | 364 C D | 1.98 | 0.76 | -7.695 | 1.79 | -0.78 | -4.03 | 3.31 | 1.91 | (0.00) | (0.00) | 53.67 |
| A6 | 364 C A | 1.98 | 0.26 | -8.245 | 2.35 | -0.70 | -7.41 | 6.86 | 3.53 | (0.00) | (0.00) | 41.37 |
| A7 | 364 D D | 2.04 | 0.80 | -7.910 | 1.68 | -1.03 | -5.76 | 4.93 | 5.46 | -18.50 | 0.89 | 34.00 |
| A7 | 364 D A | 2.04 | 0.12 | -8.360 | 1.53 | -0.81 | -3.19 | 11.00 | 4.99 | -19.50 | 22.50 | 37.00 |

# DISCUSSION

## Upper Surface Blown Flaps at 50°

The aerodynamic coefficients and stability derivatives presented in tables 1 and 2 were used to compute lift, drag, and pitching-moment curves for the aircraft at various assumed constant thrust coefficients. The curves are for the angle-of-attack ranges covered during the maneuvers and for thrust coefficients near the averages of their ranges. In figure 6 these curves are plotted for a USB flap angle of 50° and values for $C_T$ of 0.9, 1.7, and 2.2, calculated using the derivatives from the digital sets of data records from maneuvers A8, A1, and A3, respectively. In figure 7 the lift curves are compared with predictions based upon wind tunnel tests of the large scale model mentioned earlier. For the wind tunnel data, the lift coefficients were obtained at the thrust coefficients shown by interpolation, and adjustments for small differences in the flap angles are included. The slopes of the curves in this figure, i. e., the variation of $C_L$ with $\alpha$ and $C_T$, show good agreement of the flight results with the predicted variations. The wind tunnel model had no horizontal tail. The flight-measured lift curves are displaced downward because of the negative lift provided by the horizontal tail for longitudinal trim. They represent the variation of $C_L$ with angle of attack with the elevator fixed at the deflection angle at the start of the maneuver. Reference 5 shows lift curves obtained from flight measurements that have slightly less slope than those in figure 7 because they are for steady trimmed flight, for which the elevator angle varies with lift coefficient.

The pitching moment data plotted in figure 6 show that two of the curves (for $C_T$ = 0.9 and 2.2) have slopes indicating decreasing static stability as the lift increases. The other curve (for $C_T$ = 1.7) apparently did not show this characteristic only because its largest angle of attack was no larger than about 8.4°, whereas the other two reached angles exceeding 13°. Tests of the large-scale wind tunnel model mentioned earlier that has the same flap configuration but no horizontal tail showed pitching moment characteristics similar to those from the flight measurements, i.e., a forward movement of the aerodynamic center at higher angles of attack. Moment curves from the tunnel tests at two thrust coefficients, 0.9 and 1.9, are presented in figure 8. It cannot be determined from the flight data alone to what extent the decreased stability may

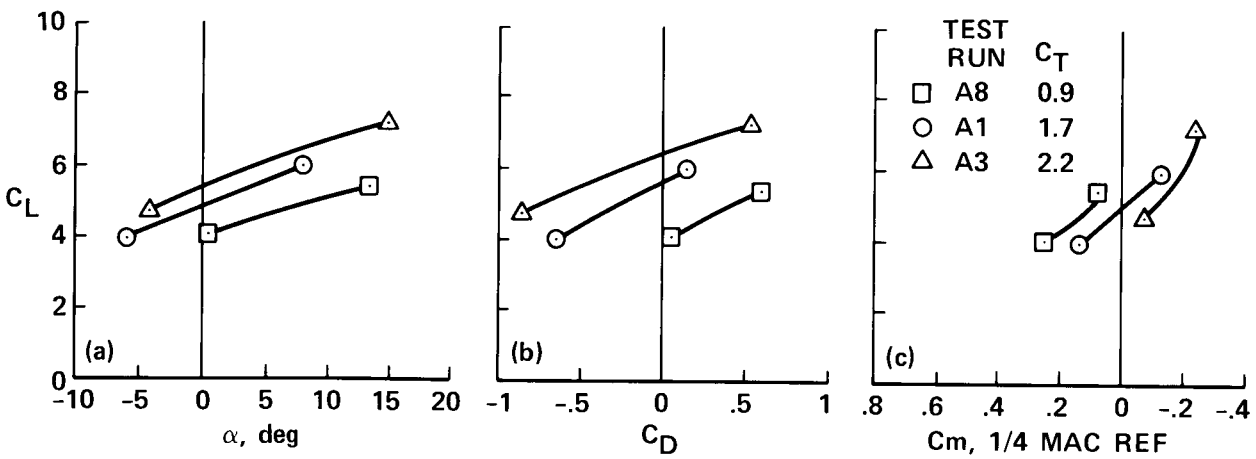


Figure 6. Lift, drag, and pitching-moment characteristics of the QSRA. USB flaps at 50°. (a) $C_L$ vs. $\alpha$; (b) $C_L$ vs. $C_D$; (c) $C_L$ vs. $C_m$.

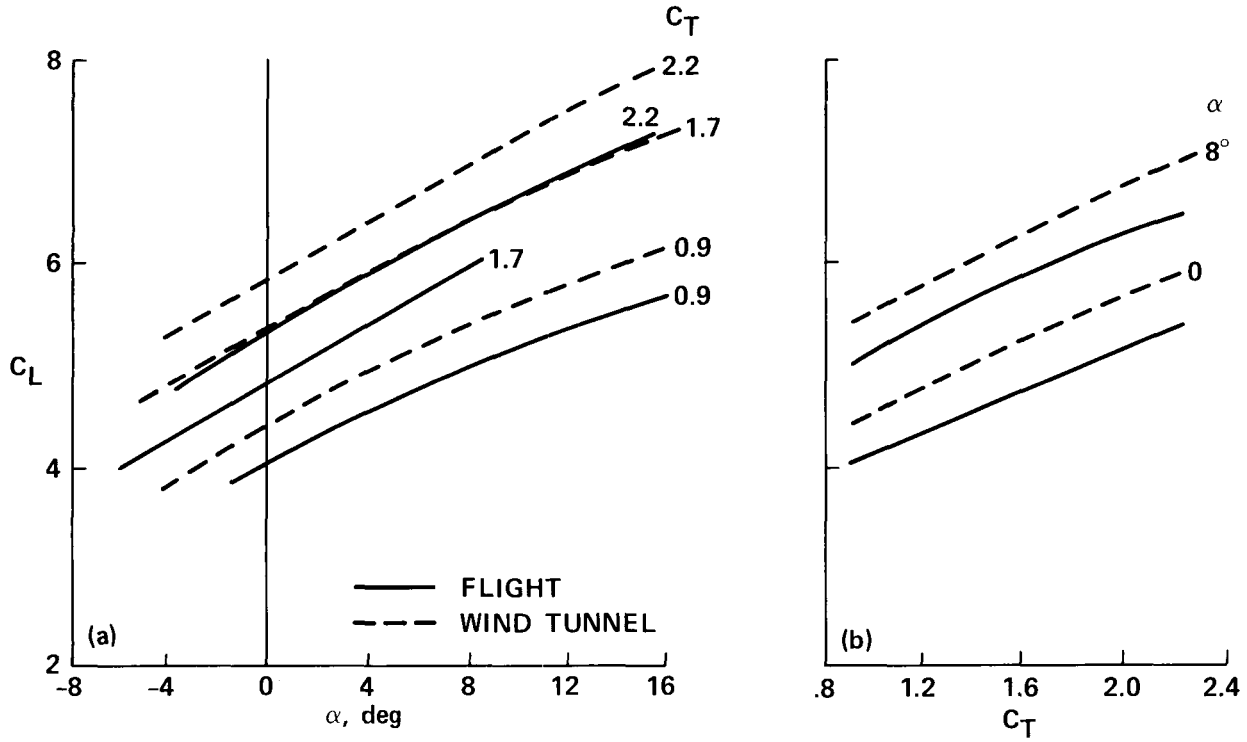


Figure 7. Lift characteristics of the QSRA compared with data from tests of a large-scale wind tunnel model. USB flaps at 50°. (a) $C_L$ vs. $\alpha$; (b) $C_L$ vs. $C_T$.

result from a change in downwash at the tail as $\alpha$ changes, but a forward movement of the a.c. of the wing and body is undoubtedly the reason for at least part of the stability change. Downwash in the region of the tail was measured with flow-angle probes in a separate study reported in reference 10. Although the downwash angles were somewhat variable with the lateral distance across the span of the tail, their slopes, $\frac{d\epsilon}{d\alpha}$, did not generally increase as the angle of attack increased. (Note that to be comparable with the present report, the data in reference 10 must be converted from the downwash variation at constant thrust to the variation at a constant thrust coefficient. Also, the wing angles of attack must be reduced by 4.5° so as to be referred to the fuselage reference line.) Other early studies aimed at determining the sources of various aerodynamic effects consisted of attaching tufts at locations on the airplane where flow separation was suspected. One observation from these studies was that under some high angle-of-attack conditions, there was separation on the rearward upper surfaces of the fuselage, which could be another contributor to the variations in static stability.

A plot of pitching-moment coefficient vs. $C_L$ at constant $C_T$ illustrates a type of static stability relating to angle-of-attack variation at constant airspeed. Another type of longitudinal static stability can be defined as the variation of $C_m$ with $C_L$ assuming that the thrust is constant and the speed varies. For aircraft which have large variations of pitching moment with thrust coefficient, such as the QSRA (with the flaps deflected), this stability can be significantly different from that for constant $C_T$. A pitching moment curve calculated in each of these two ways is plotted in figure 9, one for a thrust coefficient of 2.2 and one for a constant-thrust maneuver (for which $C_T$ varies from 1.8 to 2.6). These curves are for a USB flap angle of 50° and were computed assuming the aircraft c.g. to be at 32 percent MAC, a location in the range typical

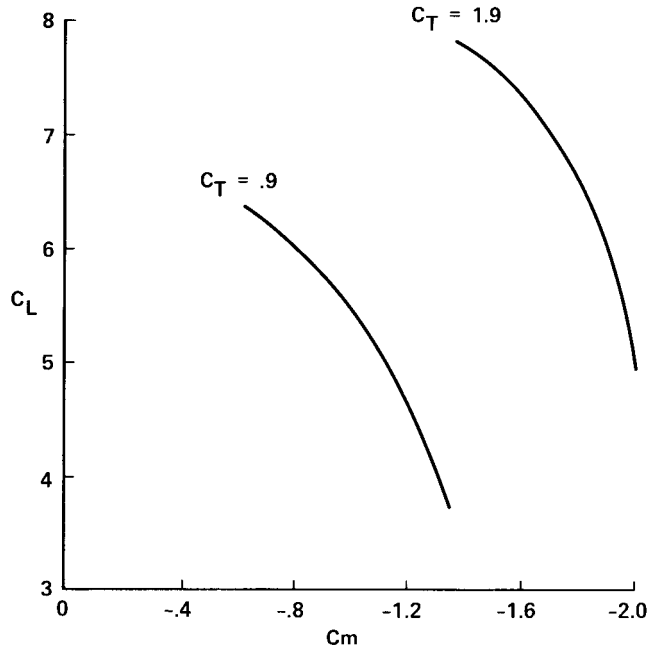


Figure 8. Pitching moment characteristics measured in wind tunnel tests of a model representing the QSRA that has no horizontal tail. USB flaps at 50°.

of the QSRA flights. The figure shows substantially greater stability when based on the constant-thrust calculation compared with that for a constant thrust coefficient.

The derivatives CZCT, CXCT, and CMCT shown in table 2 are, respectively, the variations of normal-force, axial-force, and pitching-moment coefficients with $C_T$. Within the ranges of the tests, the magnitude of CZCT decreased slightly with increasing $C_T$ and increased somewhat with angle of attack. The data show a small increase in CXCT with $C_T$, but little effect of angle-of-attack variation. Also, there was little effect on CMCT of varying either the angle of attack or the thrust coefficient.

## Upper-Surface Blown Flaps at 66°

Figure 10 presents lift, drag, and pitching-moment data from tests with the USB flaps set nominally at 66°. Throughout the angle-of-attack ranges covered in the maneuvers, this larger flap angle increased the lift at a given angle of attack and a given thrust coefficient. As with the flaps at 50°, the maneuvers were started with the airplane stabilized in steady flight at the angles of attack listed in table 1 as the initial conditions. For segments of the drag curves near these angles of attack, at a given lift coefficient, the drag is substantially greater with the USB flaps at 66° than that with the flaps at 50°. For this condition, the aircraft angle of attack is approximately 6° smaller than that for the flaps at 50°.

Figure 11 shows a comparison of the airplane's characteristics with the USB flaps at 50° and 66° at a thrust coefficient of 2.2. With the USB flaps at 66°, the moment curve does not display the decreasing static stability with increasing $C_L$ that is evident for the 50° flaps at comparable lift coefficients (but at

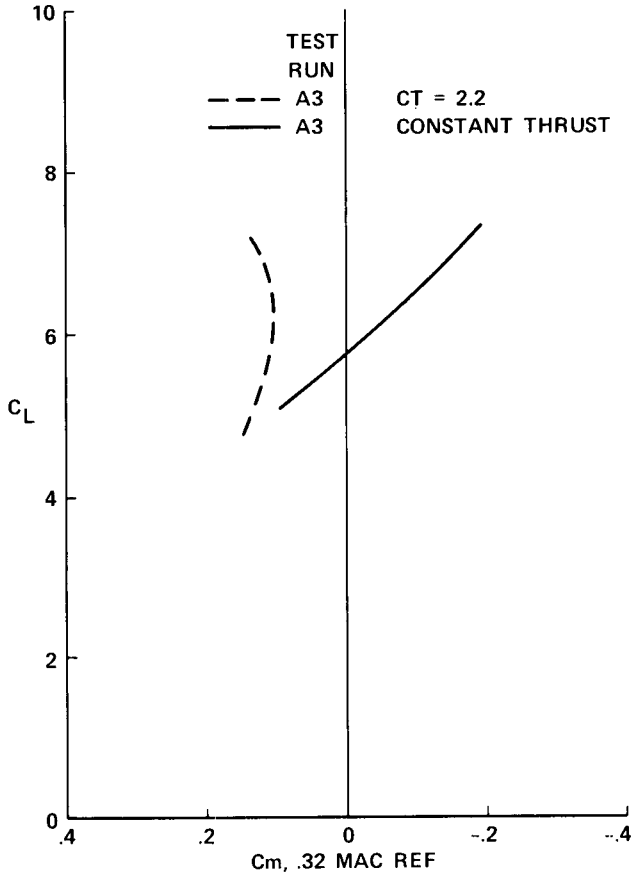


Figure 9. Comparison of pitching-moment curves calculated for constant $C_T$ and for constant thrust. USB flaps at 50°.

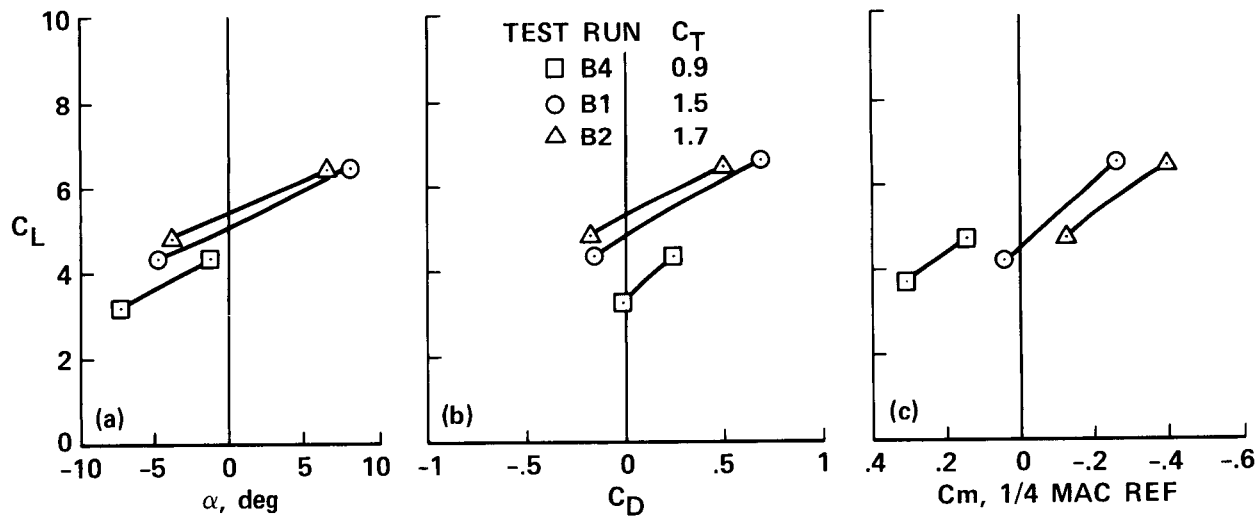


Figure 10. Lift, drag, and pitching-moment characteristics of the QSRA. USB flaps at 66°. (a) $C_L$ vs. $\alpha$; (b) $C_L$ vs. $C_D$; (c) $C_L$ vs. $C_m$.

somewhat larger angles of attack). If separation on the upper aft regions of the fuselage causes some of the instability noted above for the 50° configuration, the smaller angles of attack with the flaps at 66° would be expected to result in a reduction in the amount of separation and, as a result, less change in stability.

Table 2 shows for the 66° flap angle, the rates of change of the force and pitching-moment coefficients with $C_T$ at small angles of attack. Compared with the data for aircraft with the USB flaps at 50° and similar flight conditions, the magnitude of CZCT is greater by about 20 percent, and CXCT is smaller by about 40 percent. The magnitude of CMCT is larger than that for the 50° flap configuration by between 25 and 35 percent.

For some of the test conditions with the USB flaps at angles of both 50° and 66°, there is evidence that the elevator began to lose effectiveness, and under generally similar conditions the horizontal tail was at such large negative angles of attack that it was beginning to stall. When these effects occurred, they were noticeable in the pitching moment data as apparently anomalous variations in the static stability at high thrust levels, when the angle of attack was small. For these tests, solutions were obtained with the equations of motion modified to take these effects into account. These solutions are discussed later.

## Upper Surface Blown Flaps Undeflected

The maneuvers identified in tables 1, 2, and 4 as C1 through C6 were tests performed with the USB flaps set at zero deflection and, as before, with the slotted flaps at 59° and the ailerons drooped. Maneuvers C1, C2, and C3 began with the initial thrust levels all about the same (corresponding to values of $C_T$ between 0.58 and 0.65), but for most of test C1 the thrust coefficient was in the range from 0.35 to 0.47 because the maneuver was generated by a step reduction in thrust applied after the first few seconds. As indicated in table 1, for tests C2 and C3 the thrust coefficients were in the range from 0.58 to 0.77. Higher thrust levels were set and maintained during tests C4, C5, and C6, producing thrust coefficients ranging

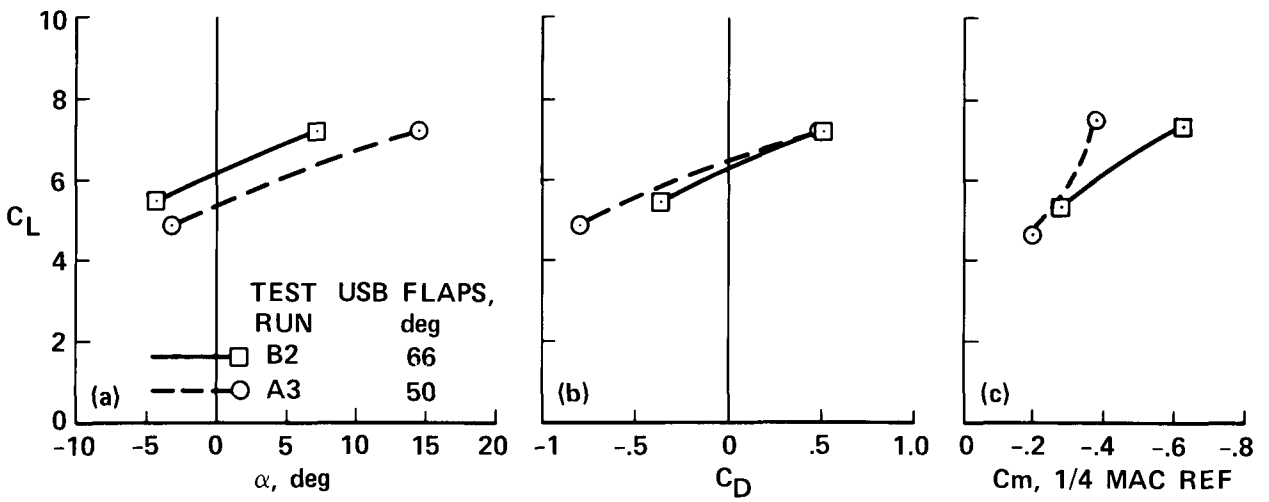


Figure 11. Comparison of the lift, drag, and pitching-moment characteristics of the QSRA, USB flaps at 66° deflection and at 50° deflection; $C_T = 2.2$. (a) $C_L$ vs. $\alpha$; (b) $C_L$ vs. $C_D$; (c) $C_L$ vs. $C_m$.

from 0.96 to 1.15 for test C4, from 1.07 to 1.39 for test C5, and from 0.55 to 1.34 for test C6, depending primarily on the ranges of the airspeeds. All of the maneuvers except C1 were responses to elevator inputs.

In figure 12 the lift, drag and pitching-moment characteristics of the aircraft in the configuration with the USB flaps undeflected at a thrust coefficient of 1.1, calculated with the data from tests C5 and C6, are compared with these characteristics calculated with data from tests done with the flaps at 50° (tests A9 and A11). An indication of the effects of thrust and angle-of-attack variation on the static stability is provided by the values for CMA and CMA2 in table 2. They indicate that the aircraft is generally less stable when the average $C_T$ is less than 0.7 (maneuvers C1, C2, and C3) than if during a maneuver, $C_T$ is 1.0 or more (tests C4, C5, and C6). Data from the three tests at the smaller thrust coefficients show negative values for CMA2, indicating that the stability increased with angle of attack. At higher thrust coefficients, the data indicate little variation of the stability with $\alpha$ within the ranges covered in the maneuvers. At angles of attack above 9°, the calculated static stability is considerably greater when the USB flaps are undeflected than when they are at 50°. Variation of the normal force coefficient with the thrust coefficient, CZCT, for the undeflected USB flaps was about the same as for the flaps at 50°, but for the axial force, the derivative CXCT is larger by a factor of two to three. The pitching-moment derivative CMCT is about one-third that for the 50° flap configuration.

A comparison of the results from the flight experiments for the aircraft with the USB flaps undeflected with those from the large-scale wind tunnel model mentioned above indicates that the variation of lift coefficient with thrust coefficient from the flight measurements is almost 30 percent greater than from the wind tunnel tests. With the USB flaps at 50°, the wind tunnel and flight results for this derivative were in fairly good agreement.

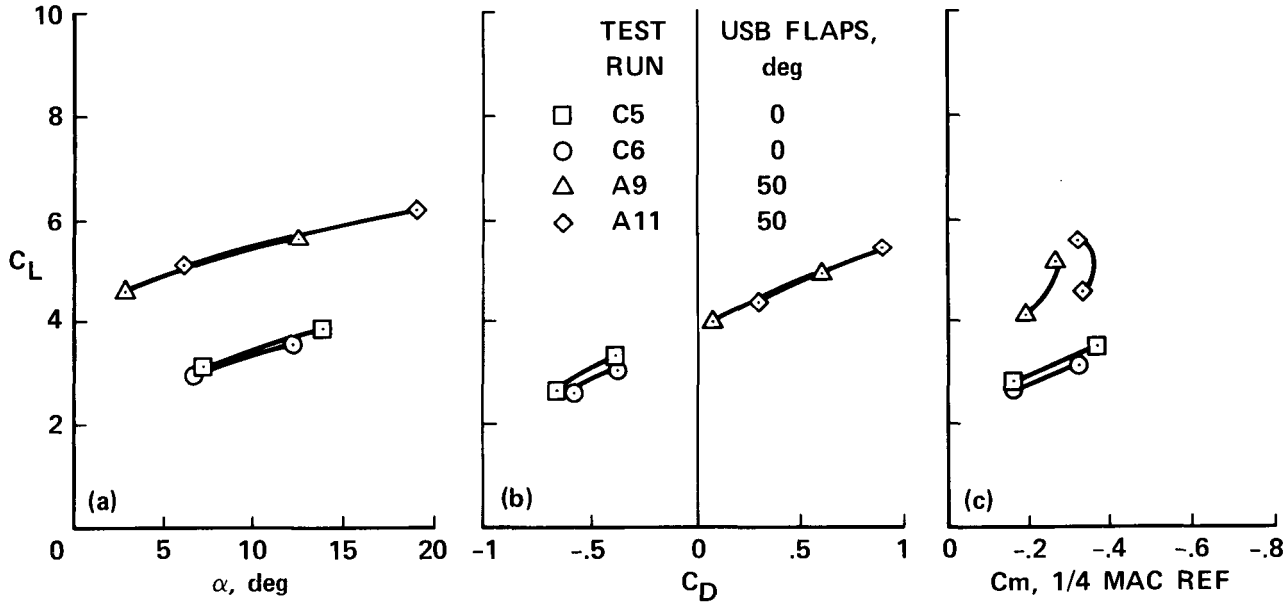


Figure 12. Comparison of the lift, drag, and pitching-moment characteristics of the QSRA, USB flaps undeflected and with 50° deflection; $C_T$ = 1.1. (a) $C_L$ vs. $\alpha$; (b) $C_L$ vs. $C_D$; (c) $C_L$ vs. $C_m$.

## Direct Lift Control Spoilers Deployed

The tests performed with the DLC spoilers set at approximately 15° and with the USB flaps at 50° are identified in the tables as D1 through D5 and E1. During test E1 only the two outer spoiler panels were deflected, whereas for these other tests all four panels were deployed. The first maneuver, D1, was a response to the pilot's application of two doublet-type displacements of the spoilers, in sequence. For maneuvers D2, D4, and D5, the inputs were positive and negative elevator pulses, and maneuvers D3 and E1 were responses to a spoiler doublet followed by elevator pulses.

Plots showing lift and drag characteristics of the aircraft with the spoilers at 15° are presented in figure 13. They were computed with data from tables 1 and 2 and are compared with data for the aircraft with the spoilers undeflected. At a thrust coefficient of 0.9 and an angle of attack of $-2°$, the spoilers produced a decrease in $C_L$ of 0.6 and a decrease in $C_D$ of about 0.04. At 10° angle of attack the data from tests D1 and D3 indicate slightly less effect on the drag and a decrease in the lift coefficient of only about 0.26. Tests of the large-scale wind tunnel model mentioned earlier indicated effects of the spoilers at angles of attack near zero that were similar to these flight results. However, at $\alpha$ near 10° the wind tunnel data indicate that the spoilers were still as effective (in decreasing $C_L$) as at small angles of attack, rather than showing the decreased effectiveness that the flight results display. At a thrust coefficient of 1.5, the data in figure 13(b), representing angles of attack from 0° to 5°, indicate a decrease in $C_L$ of about 0.46 due to the spoiler deflection and a decrease in the drag coefficient of approximately 0.05. (No wind tunnel results were available at this thrust coefficient.) Of the five maneuvers during which the four spoiler surfaces were extended, the calculations for two of them, D1 and D3, produced values for CZA and CXA that correspond to rather small values for the lift-curve slopes, significantly smaller than those for the spoilers-retracted configuration. These were the maneuvers which included spoiler doublet inputs to generate the responses. Use of this method of exciting the motion may have had an adverse effect on the accuracy of the computation of the lift-curve slopes.

A comparison of the characteristics of the airplane in steady flight with and without the spoilers extended shows a different effect when only the two outer spoiler panels are extended. Compared with data from tests A1 and A2, at a thrust coefficient of 1.4, the test with the two spoilers deployed, E1, indicates that the lift coefficient did not decrease, but was equal to or even slightly greater than the lift with the spoilers retracted. Instead of a decreasing drag coefficient, this configuration indicates that the drag coefficient was about 0.06 greater with spoilers extended. An increase in the drag is consistent with the explanation of the change in the drag at constant angle of attack being dominated by changes in the induced drag.

The static stability of the aircraft with the spoilers at 15°, computed from the two maneuvers at the higher angles of attack, D1 and D2, is similar to that with the undeflected spoiler configuration at comparable angles of attack. At small and negative values of $\alpha$, data from tests D3 and E1 indicate that as a result of the rather large negative values for CMA2 (shown in table 2), the computed static stability is sensitive to variations in $\alpha$. Within this angle of attack range, the stability is high at the larger angles, but it decreases considerably as $\alpha$ is decreased.

The three maneuvers during which the pilots actuated the DLC spoilers (D1, D3, and E1), causing their deflection angles to vary in the range from 0° to about 28°, produced responses that have been analyzed to obtain the variation of the lift, drag, and pitching-moment coefficients with the deflection angle. These

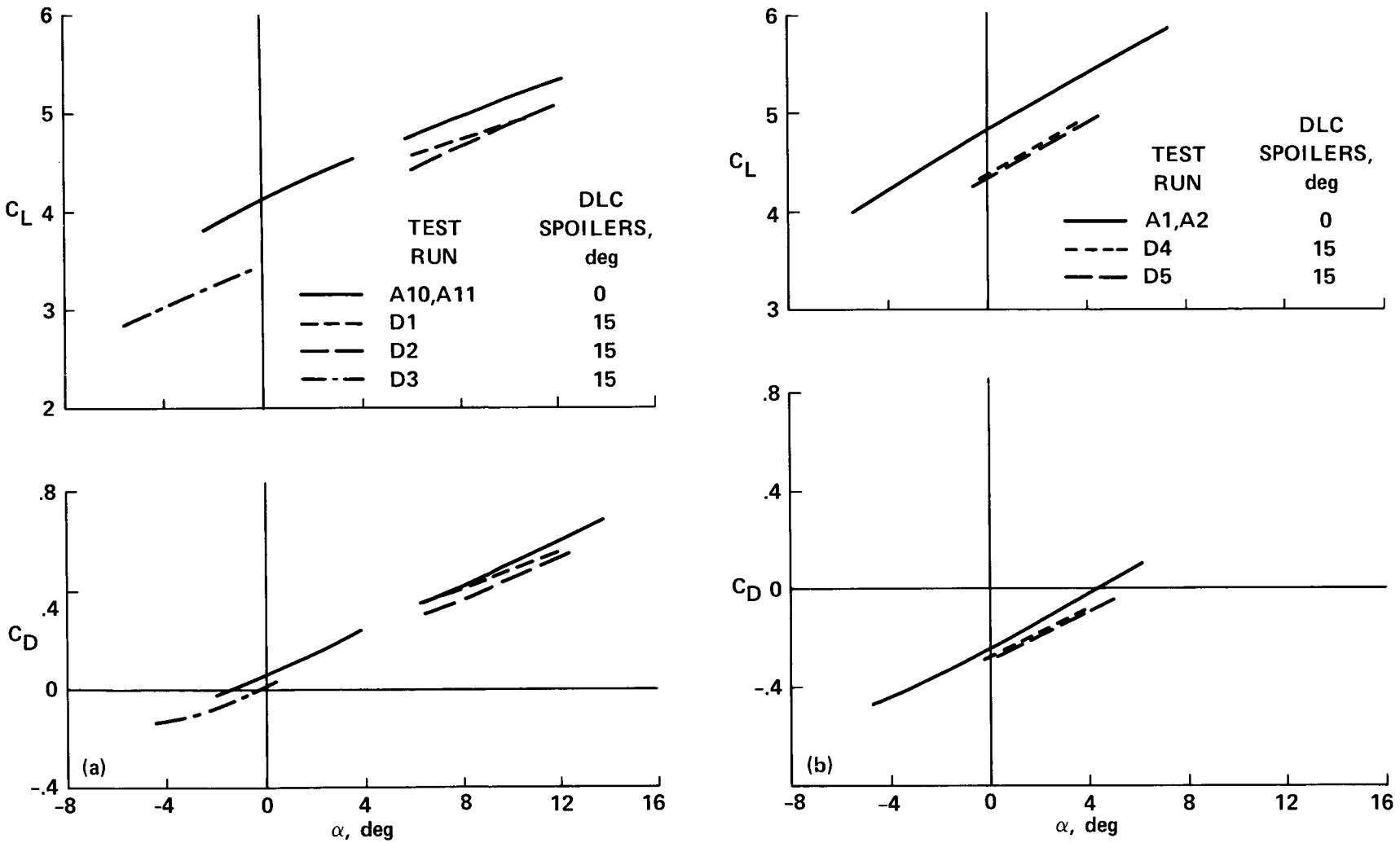


Figure 13. Lift and drag characteristics of the QSRA, DLC spoilers at 15° and 0°, USB flaps at 50°. (a) $C_T = 0.9$; (b) $C_T = 1.5$.

variations are the spoiler effectiveness derivatives, CLDS, CDDS, and CMDS, presented in table 3. Values for these derivatives are obtained from calculations in which the coefficients are assumed to vary linearly with the spoiler angle, as indicated in the equations of motion given earlier. The derivatives have been used to compute an effect on the lift of changing the angle from 0° to 15°; this effect has been compared with the effect of a change from flight with the spoilers retracted to flight with a constant 15° deflection. The values of the lift-effectiveness derivative CLDS in table 3 from test D1, in which $\alpha$ was near 10°, indicate that for a spoiler angle of 15°, there would be a decrease in the lift coefficient that is about twice that computed from the steady-flight data. If the lift increments determined from the transient response and from steady flight are compared at angles of attack represented by test D3, however, the angle of attack apparently has a significant effect. Data from test D3, for which the angle of attack ranged from about −5° to 0°, indicate that the decrease in lift coefficient due to the 15° spoiler deflection based on CLDS would be less (by about 36 percent) than that computed from the data for steady flight with the two different spoiler deflections.

The effect of spoiler deflection on the drag also depended on the angle of attack range. For $\alpha$ near 10°, the drag coefficient as computed based on the transient-response data decreased by almost twice the amount obtained from the steady-flight calculation. At small negative angles of attack, data from the transient-response portion of test D3 indicate that the drag coefficient would increase by a small amount when the spoiler angle changes from 0° to 15°, whereas the steady-flight calculations indicate that there would be a decrease by a slightly greater amount.

With only the two outboard spoilers active, the results shown in table 3 for test E1 indicate that the lift decreases with spoiler deflecton by somewhat less than that with all four panels active. This rate of decrease in lift, however, corresponds to significantly greater effectiveness than that indicated by the change in lift based on a comparison of data for steady flight with the spoiler angles of 0° and 15°.

The wind tunnel investigation indicated that the variation of lift coefficient with spoiler deflection angle was quite nonlinear, decreasing in magnitude as the angles exceeded 10°. To see if this nonlinearity would be observed in the flight results, the parameter estimation program was run with the assumption in the motion equations of a parabolic variation of the forces with spoiler deflection. These computations showed results similar to those fron the wind tunnel tests, that is, greater lift effectiveness at spoiler deflection angles less than 15°. In the case of test D3, for which the angles of attack were near 0° and lower, these calculations indicated that for spoiler deflection angles between 0° and 15°, the variation of $C_L$ with spoiler angle was essentially the same as that computed from the data for the change from zero to a constant 15° spoiler setting.

Results from tests D1 and E1 indicate that the computed response to the spoiler doublet inputs was a relatively large rate of decrease in lift with spoiler deflection, whereas the change in lift calculated as the difference in flight with constant spoiler deflection (15° and 0°) was small. No explanation for this apparent lack of agreement has been found, although there may be time-dependent effects present when the spoilers move rapidly. If the equations of motion used in the calculations include the assumption that the variation of lift with spoiler deflection is parabolic, the lack of agreement is increased.

## Elevator Effectiveness and Aerodynamic Damping

Table 4 presents the force and pitching-moment derivatives with respect to the elevator angle, pitch rate, and angle-of-attack rate $\dot{\alpha}$. There was considerable scatter in the estimated values for the derivatives CZDE and CXDE, the normal and axial forces due to elevator angle. For this reason when the data records were analyzed for most of the test maneuvers, the results shown are from calculations in which these parameters were fixed at the values indicated: $-0.7$ and $0.1$, respectively. For a few cases in which the maneuvers were excited only by variations in the thrust with very little elevator movement, a fixed value of $-3.2$ was entered for CMDE instead of including it with the estimated parameters. The majority of the estimated values for CMDE are in the range from $-3.0$ to $-3.5$, and do not show significant effects of angle-of-attack or thrust variations.

The derivatives with respect to pitch rate and to $\dot{\alpha}$ were included separately in the equations of motion, so that the effects of setting different fixed values for one or the other could be studied. Such fixed values were computed based upon the theoretical lift characteristics of the horizontal tail, estimates of the wing downwash characteristics, and upon wind-tunnel data. Sometimes, a particular choice of a value for one of these derivatives yielded sets of estimated derivatives that were judged to be better than those from other solutions. However, the values listed in the tables are considered to be significant only if the derivatives with respect to the two variables (pitch rate and $\dot{\alpha}$) are added together. Thus, in the following discussion, the sum of CMQ and CMAD, identified as $C_{m_q}$e, is considered to be the effective damping in pitch.

The pitch rate and $\dot{\alpha}$ derivatives usually cannot be separately estimated because these variables in general are correlated when the maneuvers are produced by an elevator input. Another correlation that is often observed is between the pitch rate and the elevator deflection, pointed out, for example, in reference 8. In the flight program conducted for this report, because thrust variation and the deflection of the USB spoilers during some of the tests were inputs, there are two other possible correlations: a vertical acceleration due to thrust change correlated with the angle-of-attack rate, and (during different maneuvers) the vertical acceleration due to DLC spoiler deflection, also correlated with $\dot{\alpha}$.

In figure 14, the effective pitch damping derivative $C_{m_q}$e for the airplane with the USB flaps set at 50° (tests A1 through A11) is plotted vs. the initial thrust coefficient. For most of these tests, this derivative was computed to be between $-55$ and $-75$ per radian, with no appreciable effect of variation in $C_T$ or $\alpha$. With the USB flaps set at 66°, the damping estimates from tests B2, B3, and B4 are in the same range. The larger values for the effective damping computed from both the analog and the digital data records from test B1 appear to be an effect of the correlation mentioned above between the thrust (or $C_T$) variation and $\dot{\alpha}$. This is illustrated in figure 15, which shows this damping derivative plotted against CMCT from tests B1 and B3, two tests for which the initial conditions were similar.

When the DLC spoilers were extended, the effective pitch damping was decreased to a range centered at about $-46$ per rad. The effective pitch damping estimates calculated from the digital and analog records of test D2 are noticeably larger than from the other tests for this configuration. This may be an anomaly resulting from a correlation of the pitch rate variation and the elevator angle, as evidenced by the values estimated for CMDE, which indicate greater elevator effectiveness than would be expected. A plot of this damping derivative vs. CMDE ($\frac{dC_m}{d\delta_e}$) is presented in figure 16(a). The estimated effective damping based on the analog data records from tests D1 and D3 is significantly less than that computed from the

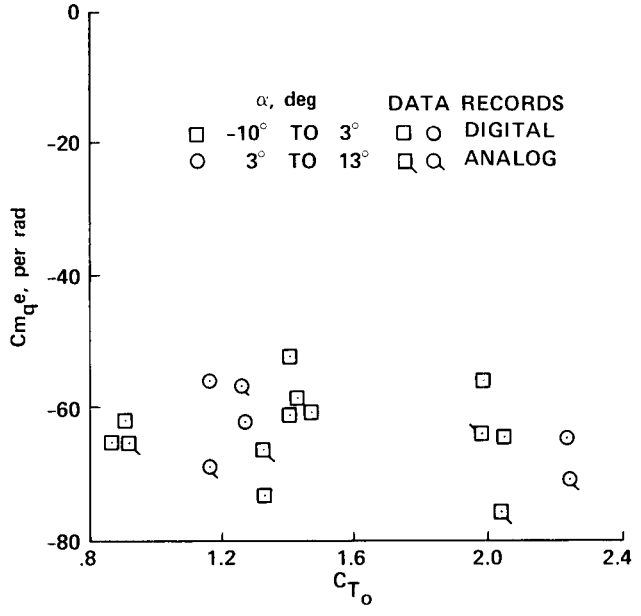


Figure 14. Effective pitch damping coefficient vs. initial thrust coefficient for the QSRA. USB flaps at 50°.

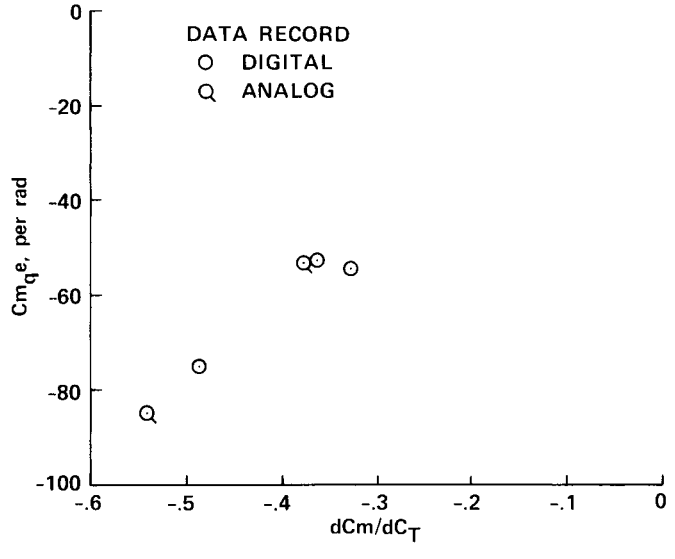


Figure 15. Effective pitch damping coefficient influenced by apparent correlation with pitching moment due to $C_T$. USB flaps at 66°; $C_T$ from 1.5 to 1.7.

digital records. This reduction appears to be due to a correlation of the spoiler deflection and $\dot{\alpha}$, having an effect primarily on the results from the analog data analysis. This is illustrated in figure 16(b), in which the effective damping derivative from these tests is plotted vs. CMDS ($\frac{dC_m}{d\delta_s}$). When the computations indicated a decreased level of damping, they yielded values for CMDS that are also smaller.

When the USB flaps were undeflected, the effective pitch damping was generally between $-50$ and $-60$ per radian, slightly less than the range for the airplane with flaps deflected. However, one test, C1, indicates very small values for this damping. It may be that the method of exciting the longitudinal motion of the aircraft for this maneuver affected the results. As mentioned earlier, maneuver C1 was generated as a response to a step decrease in thrust, whereas all the other maneuvers performed with this flap setting were responses to elevator inputs. Table 2 indicates that other results obtained from the calculations for test C1 may be anomalous. The derivatives CZA (from both the digital and the analog records) appear to be too large (in absolute magnitude) and CMA appears to be too small in magnitude to be consistent with the other results.

## Decreased Elevator and Stabilizer Effectiveness

When the USB flaps are deflected for landing approach (50° or 66°) at high thrust coefficients, large negative pitching moments must be balanced by large down loads provided by the horizontal tail. When the flaps were at the larger angle, 66°, the pilots observed situations when the elevators could not provide enough nose-up moment to maintain a level attitude, even though the speed was well above a stall. The elevators apparently were losing effectiveness due to incipient flow separation on their lower surfaces. Some comments regarding the stalling on the elevator are included in reference 11, which mentions that

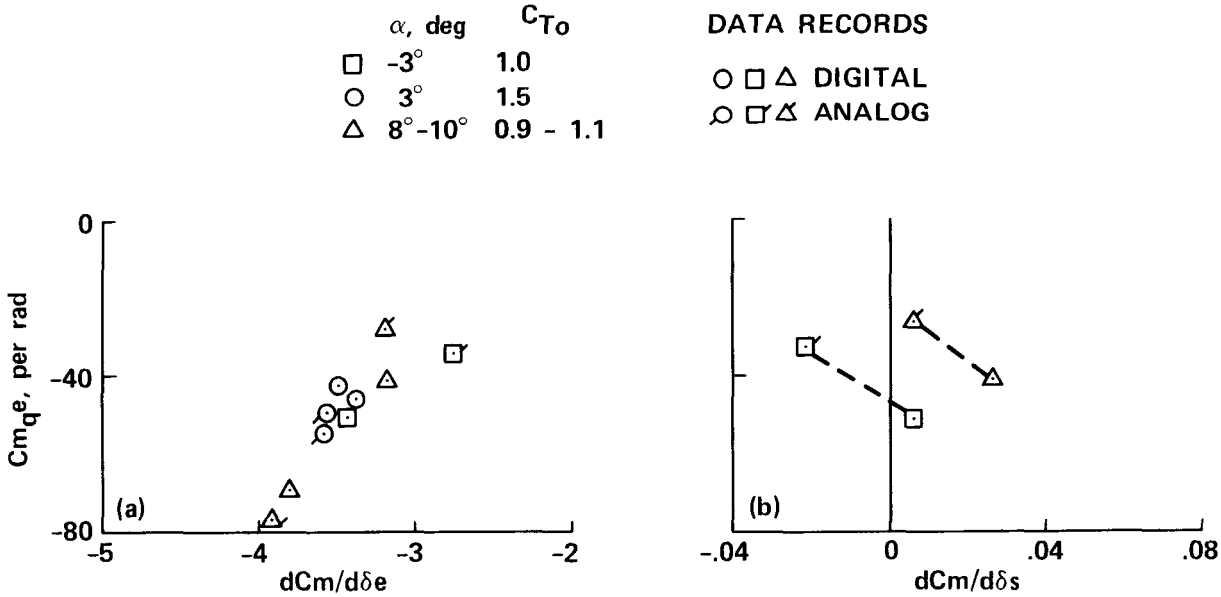


Figure 16. Effective pitch damping derivatives vs. (a) pitching moment due to elevator deflection and (b) pitching moment due to spoiler deflection. DLC spoilers, 15°. USB flaps at 50°.

the effect is observed only at the lower altitudes (below 5000 ft) and at the maximum engine power, i.e., near 89 percent rpm. The records from some of the test maneuvers performed to obtain data for this report give instances where there was also a loss in elevator effectiveness at lower levels of thrust and at a smaller USB flap angle. In these cases the elevators were being used to establish a pitch rate as well as to furnish the down load for trim. To improve the mathematical model in the parameter estimation calculations, this variation in effectiveness was taken into account by replacing the assumed linear variation of the pitching moment with elevator angle with a second order variation. Table 5 presents the results of incorporating this change in the moment equation in calculations for four maneuvers where the down load on the horizontal tail was predicted to be large. The negative values obtained for the derivative CMDE2 show that there is a significant degradation in the pitching-moment effectiveness provided by the elevators as they are deflected for nose-up control. This result indicates that there is a potential for achieving improved pitch control power by incorporating design changes such as a moveable stabilizer or provision for boundary-layer control on the elevator.

Pitching-moment curves (plots of the variation of the moment coefficient with lift coefficient at constant $C_T$) computed from the parameters shown in table 2 for the aircraft with USB flaps at 50° indicate that when the maneuvers were performed at relatively high angles of attack, the static stability decreased as angle of attack increased. Some indication of the effect of angle of attack on this stability is provided by the values of CMA2 in table 2. It can be seen that this derivative has a negative value for several of the solutions: tests A2, B2, B3, E1, and from the analog data, test A10. In these cases, the computed static stability increases with angle of attack. During these flight maneuvers, the angle-of-attack ranges were relatively small, and at some time during each test, the angle of attack decreased to negative values below $-2°$. The thrust coefficients were all relatively high. Other maneuvers covered larger angle-of-attack ranges, spanning the regions of both the negative curvature at small and negative values of $\alpha$ and the positive curvature at higher values of $\alpha$. For these cases it was evident that the assumed second degree variation of the forces and moments with angle of attack was inadequate, so a term representing a derivative with respect to the angle-of-attack increment cubed was included in the analysis of the data. Results from these maneuvers, tests A1, A3, A6, and A7, are presented in table 6. All except test A3 show fairly large values for the added pitching-moment derivative, CMA3. The smaller value for test A3 apparently occurs because the angles of attack were significantly larger initially and throughout most of the duration of the maneuver than those for the other three tests.

Figure 17 shows pitching-moment plots computed for two thrust coefficients, 1.7 (from test A1) and 2.6 (from test A7), with the parameters from table 6. The reduced static stability at low lift coefficients occurred at times of reduced normal acceleration and low airspeed. It was in effect for only a brief period of time during a push-over and evidently was not noticeable to the research pilots. It was followed by an increase in airspeed, which has the stabilizing effect of decreasing the thrust coefficient if the thrust is not increased. As in the case of the loss in elevator effectiveness, the reduced static stability is undoubtedly due to the decreased capability of the stabilizer in providing the required down load for balance, at high thrust levels and low speed. During an approach, if the thrust were to be abruptly increased to levels above the normal range, there could be a significant loss in the longitudinal control power as a result of stalling of the stabilizer and elevator. The data indicate that the increased lift capability offered by the USB flap technology could be augmented by improving the high negative lift characteristics of the horizontal tail.

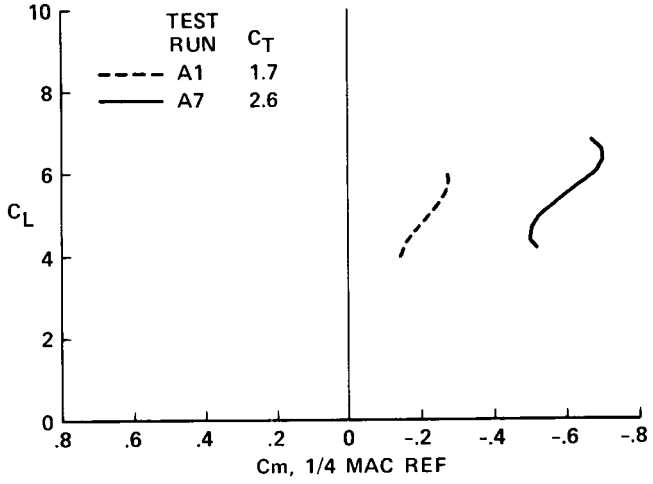


Figure 17. QSRA pitching-moment characteristics from two maneuvers which show evidence of stalling of the horizontal tail. USB flaps at 50°.

# CONCLUDING REMARKS

This report presents the results of a flight program conducted to determine performance and longitudinal stability characteristics of the QSRA, an experimental aircraft designed and built to study the application of the upper-surface blown (USB)-flap powered-lift concept. Time-history records were obtained from flight maneuvers performed with the aircraft in landing-approach and take-off configurations, which covered a large range of engine thrust levels and angles of attack. All of the tests were done with the stability augmentation system of the aircraft disengaged. The records were analyzed with a linear regression parameter estimation procedure to extract longitudinal stability and control derivatives.

The static stability derivatives were used to calculate lift, drag, and pitching-moment curves for various constant thrust coefficients selected to represent the conditions of the particular maneuvers. The lift characteristics of the aircraft in a landing configuration from these calculations show good agreement with the lift characteristics predicted for the aircraft based on tests of a large scale wind-tunnel model.

Pitching-moment data for the aircraft in one landing approach configuration, in which the USB flaps were deflected 50°, indicate that as the angle of attack is increased above about 9°, there is a significant decrease in the magnitude of the static longitudinal stability derivative, $\frac{dC_m}{d\alpha}$. This change in stability was not evident in data obtained with the USB flaps set at 66° at similar lift coefficients. The larger flap angle provided higher lift coefficients at a given angle of attack, but also resulted in a considerable increase in the drag. Results from tests with the USB flaps undeflected, representing a take-off configuration, also did not indicate a decrease in the static stability as the angle of attack increased within the range covered, up to about 14°.

The aircraft has the capability to control its flightpath angle by setting direct-lift-control spoilers at a reference angle of deflection, from which they can be driven to angles from zero to about 28°. The aerodynamic characteristics of the airplane with the spoilers at a reference angle of approximately 15° and with the USB flaps set at 50° were investigated. Compared with results for the aircraft with spoilers retracted, there was a significant decrease in lift for the same $\alpha$ and $C_T$, but the decreases differed considerably at different angles of attack and thrust coefficients. Deflecting the spoilers to 15° decreased the drag coefficient at a constant angle of attack because of the large decrease in the induced drag. In addition to this determination of the characteristics of the aircraft with a fixed spoiler deflection, transient responses to spoiler deflections were recorded during portions of maneuvers in which the pilots applied doublet type inputs, moving them rapidly between 0° and 28°. The decrease in lift coefficient for a 15° spoiler deflection, calculated on the basis of the transient measurements (assuming a linear variation of lift and drag with deflection angle), at an angle of attack of 10°, is about twice that computed from the fixed-deflection data. At small negative angles of attack, this decrease is less than that computed from the fixed-spoiler tests.

When the QSRA operates at high levels of thrust and relatively low airspeed in a landing approach configuration, a large negative lift on the horizontal tail is required for trim. During some of the test maneuvers under these conditions, additional down load on the tail was applied for nose-up pitch control. For some tests the data indicate that the elevator was losing effectiveness as a result of lower-surface stalling. An estimate of this change in effectiveness was obtained by including in the equations of motion for the aircraft the assumption that the variation of pitching moment with elevator deflection was a parabolic function. Some of the pitching moment curves, $C_m$ vs. $C_L$, plotted for conditions where large down

loads on the stabilizer are expected, indicated that the magnitude of the static stability derivative of the aircraft decreased as the angle of attack decreased to zero and negative values. This effect is attributed to a beginning of a stall on the entire horizontal stabilizer. There were several test maneuvers that showed evidence of this decreased stability at small $\alpha$, but during the maneuvers at times relatively large angles of attack were attained. In these cases, it was found that the mathematical model for the motion was improved by assuming that the pitching moment variation with angle of attack was a third order function, such that at some point the curvature of the moment curve could change sign.

# APPENDIX

# DATA REDUCTION

Corrections to aerodynamic data that were applied as part of the data reduction are taken from tests conducted prior to those that are the subject of this report. The vane indicated angle of attack, $\alpha_i$, was corrected by adding the increment $\Delta\alpha$, given by the following formula, in degrees.

$$\Delta\alpha = -1.5[1. + 0.0182(\delta_u - 55.)] - 0.12[1. + 1.5(\delta_u - 55.) + 0.0108(N - 60.)]\alpha_i$$
$$- 0.0021\alpha_i^2 \tag{7}$$

where $\delta_u$ is the USB flap deflection angle in degrees and $N$ is the engine fan percent rpm, averaged among the engines.

Pitot static data corrections had been determined from low level flights in calm air under conditions where the true speed could be measured and the air density was known. The following formula was used to compute a correction which was added to the indicated airspeed ($V_i$) in knots.

$$\Delta V = 0.3219 \times 10^{-4} V_i^3 - 0.01231 V_i^2 + 1.4762 V_i - 53.405 \tag{8}$$

The corrected dynamic pressure ($\bar{q}$) was calculated from the equation, in $lb/ft^2$

$$\bar{q} = 0.003385 V_i^2 (1. + \Delta V(2. + \Delta V/V_i^2)/V_i) \tag{9}$$

The corrected static pressure ($P_s$) was computed from the indicated pressure ($P_i$) with the relation

$$P_s = P_i - 0.003385 \Delta V (2. + \Delta V/V_i) \tag{10}$$

The expression below was determined to be a suitable representation of the engine thrust as a function of fan percent rpm, Mach number $M$, ambient pressure ratio, and temperature. Defining $T_r$ as the ratio of absolute ambient to sea-level standard temperature and

$$P_r = P_s/2116.15$$
$$N_t = N/\sqrt{T_r}$$

for one engine the thrust $T_n$ was computed as

$$T_n = P_r[(1.134 + 0.78 M^2) N_t^2 - (53.3 + 27.M^2) N_t + 6430 M^2 + 1420] \tag{11}$$

The thrust coefficient for the four engines is calculated as

$$C_T = \sum_{n=1}^{4} \frac{T_n}{\bar{q} S}$$

The mass flow rate $\dot{M}$ of the air entering the engines was computed from the thrust and pressure ratio in slugs per sec as follows.

$$\dot{M} = \frac{P_r}{\sqrt{T_r}}[0.4911 \times 10^{-9}(T_n/P_r)^2 + 0.00119(T_n/P_r + 2.5)] \tag{12}$$

The ram drag coefficient was calculated from the following relations, in which $V_t$ is the true airspeed in feet per second and the mass flow is summed for the four engines.

$$V_t = 29.03\sqrt{(T_r\,\bar{q})/P_r}$$

$$C_{D_R} = \frac{V_t}{\bar{q}\,S}\sum_{n=1}^{4}\dot{M}_n$$

In the drag and moment data presented in this report, the ram drag effect has been removed.

The longitudinal and normal accelerations in the equations of motion are at the aircraft c.g. The accelerometer package was located in the horizontal plane of the c.g., 1.45 ft behind the quarter-chord point of the mean aerodynamic chord and 0.71 ft to the left of the plane of symmetry. The quantities $X_a$ and $Y_a$ which in the equations below represent the distances of these instruments from the c. g. for the test conditons are negative in sign. Accelerations were transferred to the c. g. with the equations

$$a_Z = a_{Z_i} + (X_a(\dot{q} - pr) - Y_a(qr + \dot{p}))/g \tag{13}$$

and

$$a_X = a_{X_i} + (X_a(q^2 + r^2) - Y_a(pq - \dot{r}))/g \tag{14}$$

where $a_{X_i}$ and $a_{Z_i}$ are the instrument measurements.

Prior to the application of the parameter estimation program (ref. 9) the data records were smoothed and filtered with the preprocessing program as described by R. E. Bach, Jr. in "State Estimation Applications in Flight-Data Analysis (A User's Manual for SMACK)" (NASA RP, to be published). In Bach's report, the program is employed for preprocessing data before executing a state estimation analysis. This preprocessing included the determination of the time derivatives of the measured angular rates to obtain the angular accelerations required in the equations of motion.

# REFERENCES


1. Franklin, J. A.; Hynes, C. S.; Hardy, G. H.; Martin, J. L.; and Innis, R. C.: Flight Evaluation of Augmented Controls for Approach and Landing of Powered-Lift Aircraft. AIAA J. Guidance, Control, and Dynamics, vol. 9, no. 5, Sept.-Oct. 1986.

2. Boeing Commercial Airplane Company Staff: Quiet Short-Haul Research Aircraft Phase II Flight Simulation Mathematical Model–Final Report. NASA CR-152197, Sept. 1979.

3. Aoyagi, K.; Falarski, M. D.; and Koenig, D. G.: Wind Tunnel Investigation of a Large-Scale Upper Surface Blown-Flap Model Having Four Engines. NASA TM X-62,419, July 1975.

4. Cochrane, J. A.; Riddle, D. W.; and Stevens, V. C.: Quiet Short-Haul Research Aircraft—The First Three Years of Flight Research. AIAA Paper 81-2625, 1981.

5. Stevens, V. C.: A Technique for Determining Powered-Lift STOL Aircraft Performance at Sea Level from Flight Test Data Taken at Altitude. 13th Annual Symposium of the Society of Flight Test Engineers, Sept. 1982.

6. Riddle, D. W.; Stevens, V. C.; and Eppel, J. C.: Quiet Short-Haul Research Aircraft—A Summary of Flight Research Since 1981. SAE Paper 872315, International Powered-Lift Conference, Dec. 1987.

7. Riddle, D. W.; Innis, R. C.; Martin, J. L.; and Cochrane, J. A.: Powered-Lift Takeoff Performance Characteristics Determined from Flight Test of the Quiet Short-Haul Research Aircraft (QSRA). AIAA Paper 81-2409, 1981.

8. Gerlach, O. H.: The Determination of Stability Derivatives and Performance Characteristics from Dynamic Maneuvers. Report VTH-163, Delft Univ. of Technology, March 1971.

9. Bach, R. E., Jr.: A User's Manual for AMES (A Parameter Estimation Program). NASA CR-163118, 1974.

10. Eppel, J. C.; Riddle, D. W.; and Stevens, V. C.: Flight Measured Downwash of the QSRA. AIAA Paper No. 88-2141, AIAA Fourth Flight Test Conference, May 1988.

11. Cochrane, J. A.; Riddle, D. W.; Stevens, V. C.; and Shovlin, M. D.: Selected Results from the Quiet Short-Haul Research Aircraft Flight Research Program. AIAA J. Aircraft, vol. 19, no. 12, Dec. 1982.

NASA
National Aeronautics and Space Administration

# Report Documentation Page

| 1. Report No. | 2. Government Accession No. | 3. Recipient's Catalog No. |
|---|---|---|
| NASA TP-2965 | | |

| 4. Title and Subtitle | 5. Report Date |
|---|---|
| Longitudinal Stability and Control Characteristics of the Quiet Short-Haul Research Aircraft (QSRA) | December 1989 |
| | 6. Performing Organization Code |

| 7. Author(s) | 8. Performing Organization Report No. |
|---|---|
| Jack D. Stephenson and Gordon H. Hardy | A-89133 |
| | 10. Work Unit No. 505-61-71 |

| 9. Performing Organization Name and Address | 11. Contract or Grant No. |
|---|---|
| Ames Research Center<br>Moffett Field, CA 94035 | |
| | 13. Type of Report and Period Covered<br>Technical Paper |

| 12. Sponsoring Agency Name and Address | 14. Sponsoring Agency Code |
|---|---|
| National Aeronautics and Space Administration<br>Washington, DC 20546-0001 | |

15. Supplementary Notes

Point of Contact: Gordon H. Hardy, Ames Research Center, MS 211-3, Moffett Field, CA 94035
(415) 694-3129 or FTS 464-3129

16. Abstract

Flight experiments have been conducted to evaluate various aerodynamic characteristics of the Quiet Short-Haul Research Aircraft (QSRA), an experimental aircraft that makes use of the upper-surface blown (USB) powered-lift concept. Time-history records from maneuvers performed with the aircraft in landing-approach and take-off configurations (with its stability augmentation system disengaged) were analyzed to obtain longitudinal stability and control derivatives and performance characteristics. The experiments included measuring the aircraft responses to variations in the deflection of direct-lift-control spoilers and to thrust variations, as well as to elevator inputs. The majority of the results are given for the aircraft in a landing configuration with the USB flaps at 50°. For this configuration, if the static longitudinal stability is defined as the variation of the pitching-moment coefficient with the lift coefficient at a constant thrust coefficient, this stability decreases significantly with increasing angle of attack above 9°. Also, for this configuration, at small and negative angles of attack and high levels of thrust, the elevators and the horizontal stabilizer lost effectiveness owing to incipient stalling, but this occurred only during unsteady maneuvers and for brief time intervals.

| 17. Key Words (Suggested by Author(s)) | 18. Distribution Statement |
|---|---|
| Aircraft stability, STOL aircraft,<br>Flight research, QSRA aircraft,<br>Longitudinal stability | Unclassified-Unlimited<br><br>Subject Category - 08 |

| 19. Security Classif. (of this report) | 20. Security Classif. (of this page) | 21. No. of Pages | 22. Price |
|---|---|---|---|
| Unclassified | Unclassified | 44 | A03 |

NASA FORM 1626 OCT 86

For sale by the National Technical Information Service, Springfield, Virginia 22161

NASA-Langley, 1989